Photochemical Rearrangement of a 19-Membered Azoxybenzocrown: Products and their Properties

Ewa Wagner-Wysiecka,[a] Paulina Szulc,[a] Elżbieta Luboch,*[a] Jarosław Chojnacki,[b] Katarzyna Szwarc-Karabyka,[c] Natalia Łukasik,[a] Miłosz Murawski,[a,d] and Michał Kosno[a,e]

[a]*Department of Chemistry and Technology of Functional Materials,* [b]*Department of Inorganic Chemistry,* [c]*Nuclear Magnetic Resonance Laboratory,* [d]*Present address: Department of Physical Chemistry,* [e]*Present address: Department of Pharmaceutical Technology and Biochemistry,*
Faculty of Chemistry, Gdańsk University of Technology, Narutowicza Street 11/12, 80-233 Gdańsk, Poland
e-mail address: elzluboc@pg.edu.pl

Abstract

The preparation and characterization of products of the chemical and photochemical rearrangements of a 19-membered *o*,*o*'-azoxybenzocrown were presented. In photochemical rearrangement, besides expected product i.e. 19-membered *o*-hydroxy-*o*,*o*′-azobenzocrown (**19-*o*-OH)**, obtained under defined conditions with 75% yield, also other macrocyclic products were isolated and identified, namely: 19-membered *p*-hydroxy-*o*,*o*′-azobenzocrown (**19-*p*-OH)**, 21-membered *o*′-hydroxy-*o*,*p*′-azobenzocrown (**21-*o*′-OH)** and 19-membered macrocycle containing 5-membered ring bearing an aldehyde group (**19-al)**. The structures of two atypical products of the photochemical rearrangement - **21-*o*′-OH** and **19-al** - were determined in the solid state by the X-ray method and in solution using NMR spectroscopy. Tautomeric equilibrium of the formed hydroxyazobenzocrowns and its change depending on acidity/basicity of the environment and alkali and alkaline earth metal cations complexation

were studied using UV-Vis spectrophotometry, spectrofluorimetry and ^{1}H NMR spectroscopy.

Introduction

Azobenzene is one of the most often introduced chromophores into more complex molecules [1,2] including macrocyclic compounds, where it can consist both a peripheral or an inherent part of the molecule.[3,4] Macrocyles with an inherent azobenzene fragment substituted in *o*,*o*′- positions of benzene rings with polyether linkage (azobenzocrowns, Figure 1) combine the properties of azobenzene and crown ethers, e.g. metal cation complexation according to their size, connected with spectral changes in the visible range of the electromagnetic spectrum.[4-6] On the other hand, lipophilic derivatives of azobenzocrowns can be used as ionophores in membrane ion-selective electrodes.[3,4] An interesting functionality introduced into the azobenzocrown skeleton is the hydroxyl group (Figure 1), which can be located in the benzene ring in the *ortho* or *para* position to the azo moiety.[7-12]

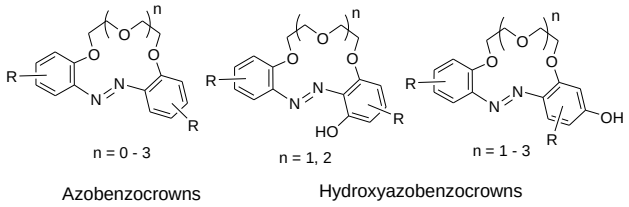

Figure 1. Azobenzocrowns and hydroxyazobenzocrowns.[5-12]

Macrocyclic hydroxyazocompounds can be obtained in various procedures.[8-12] One of them is chemical transformation of azoxycompounds leading mainly to *p*-hydroxyazocompounds, known as the Wallach rearrangement.[14] The process occurs in a strong acid environment (also Lewis acids) but sulfuric acid has been found to be the most effective.[17] It was also reported, that solid acidic catalysts can promote transformations of azoxy compounds towards hydroxy derivatives.[18] *Ortho* isomers can be expected to form in small quantities or in preferential quantities especially when *para* position(s) in the azoxybenzene skeleton is (are) occupied.[8,15,16] Since the first reports of azoxyarenes transformation to hydroxy derivatives a lot of work has been done to study the nature of this rearrangement.[19-25] The studies of the mechanism with ^{18}O isotope labeled sulfuric acid proved, that the Wallach rearrangement is an intermolecular process.[26]

The transformation of azoxybenzene to hydroxyazobenzene can also occur under photo illumination. Sometimes this process is referred as the photo-Wallach rearrangement.

In the photochemically driven process the final product is formed as a result of the intramolecular migration of the oxygen atom to the more distant aromatic ring connected to the nitrogen atom, resulting in formation of *o*-hydroxyazoarenes.[27] The mechanism of this reaction was examined for simple azoxycompounds by Badger and Buttery.[27] Lewis and Reiss[28] found the presence of additional, atypical products of the photo rearrangement of 2,2′- dimethylazoxybenzene. Other valuable, original contributions and reviews discussing and debating on the possible mechanism of photo rearrangement of azoxyarenes are also worth mentioning here.[6,19, 29-36]

A reaction analogous to the Wallach rearrangement with azoxybenzocrowns as substrates was proposed as one of the possible preparation methods of *p*-hydroxyazobenzocrowns.[8,10,11] Under optimized conditions (acid concentration, type of solvent, time, temperature) successful synthesis of 13- and 16-membered *p*-hydroxyazobenzocrowns was carried out (Scheme 1, n = 1, 2) resulting in 78 and 72% yield for **13-*p*-OH** and **16-*p*-OH**, respectively.

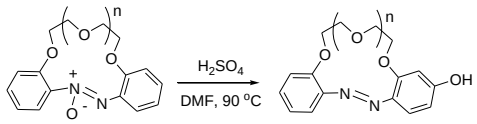

1a. n=1
2a. n=2

13-*p*-OH n=1
16-*p*-OH n=2

Scheme 1. Synthetic route for preparation of *p*-hydroxyazobenzocrowns in a reaction analogous to the Wallach rearrangement.[8,10,11]

Photochemical reactions were also found to be a promising way for the preparation of macrocyclic hydroxyazobenzocompounds.[11] The preliminary studies on the photochemical rearrangement of 13- and 16-membered azoxybenzocrowns indicated that process results in formation of a mixture of hydroxyazobenzocrowns. Two main products were isolated: *ortho*- and *para*- hydroxyazobenzocrowns. The ratio of the *para* to *ortho* isomer is dependent on the type of solvent. In toluene, *o*-substituted compounds were dominating, *p*-substituted crowns were the main products in ethanol. In DMF a mixture, containing almost equal amounts of both isomers, is formed. Under photochemical reaction conditions *trans-cis* isomerization of azoxybenzocrowns was also observed. *Cis* isomers of azoxycompounds were characterized.[11]

Until now, 19-membered *p*-hydroxyazobenzocrown **19-*p*-OH** (Figure 1, n = 3) has been obtained only in the direct synthesis, namely stannite reduction of hydroxydinitropodand. A multistep procedure, with protection of the hydroxyl group gave *p*-hydroxyazobenzocrown without a satisfying yield.[7]

Here we present the preparation and characterization of the products of the chemical and photochemical rearrangements of a 19-membered azoxybenzocrown. The structures of two atypical products of the photochemical rearrangement were determined in the solid state by the X-ray method and in solution using NMR spectroscopy. The tautomeric equilibrium of obtained hydroxyazobenzocrowns and its change depending on acidity/basicity of the environment and alkali and alkaline earth metal cations complexation were studied using UV-Vis spectrophotometry, spectrofluorimetry and ^{1}H NMR spectroscopy.

Results and discussion

Chemical and photo-driven transformations of a 19-membered azoxybenzocrown

The 19-membered *p*-hydroxyazobenzocrown **19-*p*-OH** was now obtained in a reaction analogous to the Wallach rearrangement (Scheme 2). The procedure was similar to that described earlier for 13- and 16-membered hydroxyazobenzocrowns,[11] using the 19-membered azoxybenzocrown **19-AZB-O**.[37] In this way, under optimized conditions, **19-*p*-OH** was obtained with the highest, among all prepared until now hydroxyazobenzocrowns, yield of 82%. Other macrocyclic products of this reaction have not been isolated so far. Small quantities of azobenzocrown (**19-AZB**) were identified using chromatographic methods (TLC).

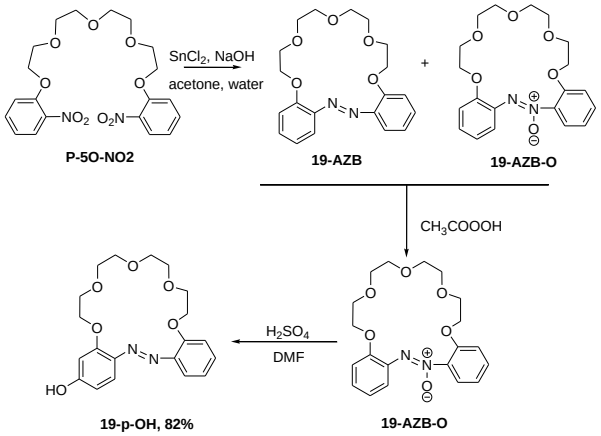

Scheme 2. Synthetic route for preparation of **19-AZB-O** and for preparation of **19-*p*-OH** in a reaction analogous to the Wallach rearrangement.

Regardless of the reaction analogous to the Wallach rearrangement, a number of photochemical rearrangement reactions for **19-AZB-O** was carried out. The composition of the resulting post-reaction mixtures was analyzed in detail (Scheme 3).

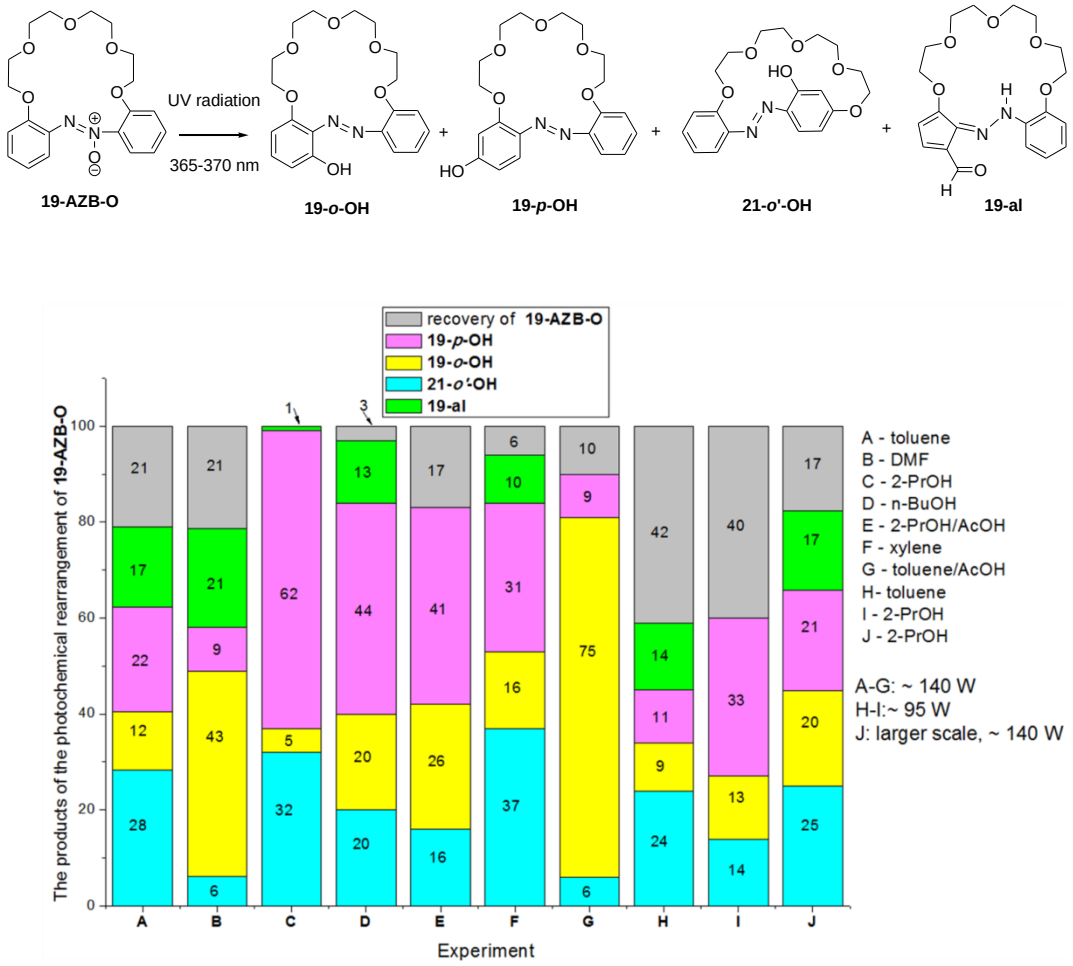

Scheme 3. The photochemical rearrangement of 19-membered azoxybenzocrown **19-AZB-O** and comparison of the reaction yield given as percent of isolated individual compounds, depending on the solvent and conditions.

The course of the photochemical reaction, i.e. the overall yield of macrocyclic compounds, distribution ratio of products and substrate recovery, was studied. Under the established experimental conditions (Scheme 3): power ~ 140 W, UV light 365-370 nm, ~35 mg of substrate in ~65 mL of solvent (the concentration of substrate did not exceed $1.4 \cdot 10^{-3}$ mol·L^{-1}) an influence of solvents of different properties (experiments A-G), also with a small addition of acetic acid was investigated. Another parameter influencing the photochemical rearrangement of the substrate was the power of the UV light (experiments H, I). One experiment, namely J, was carried out in a larger scale. Details concerning inputs are collected in Experimental. The highest (≥90%) conversion of azoxycompound to isolated and

identified products **19-*o*-OH**, **19-*p*-OH, 21-*o*′-OH**, and **19-al** (at UV power of about 140 W) was found to be solvent dependent and can be put in the order: 2-propanol>n-butanol>xylene>toluene/acetic acid mixture.

Photochemical rearrangement of **19-AZB-O** resulting in obtainment of **19-*o*-OH** seems to be favored in DMF (among all investigated neutral solvents). The beneficial effect of acetic acid addition is well seen in reactions carried out in toluene (the increase of yield of **19-*o*-OH** from 12 to 75%). The positive effect of the presence of acetic acid or solid acid catalyst in photo-driven formation of *o*-hydroxyazocompounds was also reported by other authors.[18, 34, 36]

In case of **19-*p*-OH**, the highest, 62% yield was found in 2-propanol - a polar, protic, hydrogen bonding solvent (Scheme 3, experiment C). The relatively high yield of *p*-hydroxyazocompound is distinctive in all cases, where alcohols were used as solvent. It is worth noting that in alcohols in the presence of acetic acid the yield of *p*-hydroazoxycrown is lower, with a higher yield of the 19-membered *ortho* isomer.

The formation of *o*- and *p*-hydroxyazobenzocrowns **19-*o*-OH** and **19-*p*-OH** can be more or less easily explained on the basis of exhaustive studies carried out for different type of azoxycompounds by other authors cited in the Introduction. Interestingly, among the isolated reaction products, macrocyclic 21-membered compound **21-*o*′-OH** with an inherent, e.g., directed towards molecular cavity, *o*-hydroxyl group, in which benzene rings are *o*,*p*′-substituted with an oligoether chain, was identified. The formation of this product was found in all experiments, but the highest yield was noticed in xylene. The unexpected products of rearrangement of azoxycompounds both in chemical and photo stimulated reactions have been also reported in the literature.[22,30]

On the basis of literature data on photochemical rearrangement of azoxybenzene and its derivatives we suggest the formation of **19-*o*-OH** and **21-*o*′-OH** according to Scheme 4. The intermediate **A**, proposed by Lewis and Reiss,[28,30-32] is well accepted as leading to the formation of *o*-hydroxyazocompounds, here **19-*o*-OH**. According to Bunce,[30] an eventual migration of hydride in **A** should be easy, what could give another intermediate **B**, also leading to *o*-hydroxyazocompound. In the case of azoxybenzene derivatives, the presence of base, even a very weak one, favors the formation of typical *ortho*-derivatives. In the absence of base the generation of diazonium cation from **B** is probable, resulting in formation also atypical for photochemical rearrangement hydroxyazocompounds, here for example **21-o′-OH**, as an effect of diazonium coupling reaction.

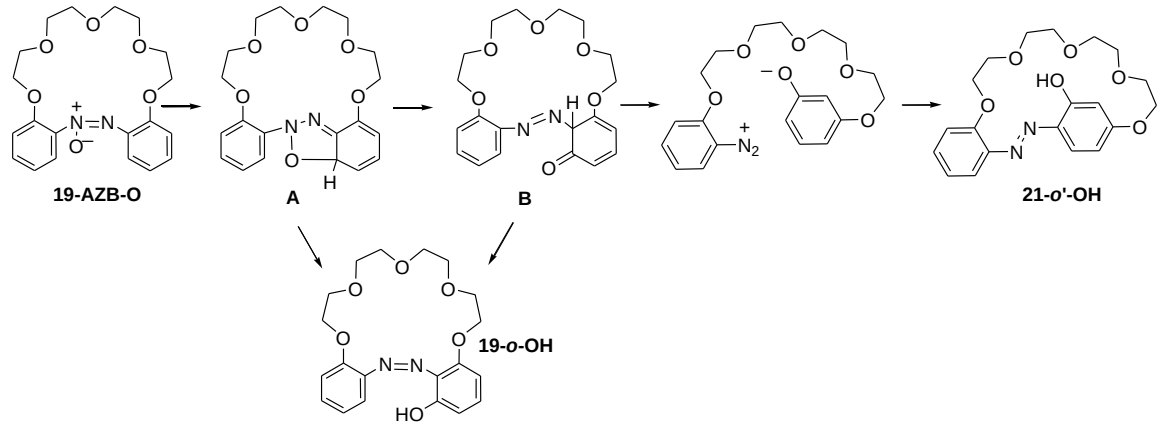

Scheme 4. Photochemical rearrangement of **19-AZB-O**: the proposed course of formation of **21-*o′*-OH** and **19-*o*-OH**.

In the photochemical rearrangement one more, untypical product was isolated and identified. It is a compound labeled as **19-al** (Scheme 3) originating probably from the contraction of the six-membered ring as a result of alternative transformation of by-product **A** (Scheme 4). The formation of 5-membered aromatic ketoderivatives, but from chlorophenols under UV illumination, was reported in the literature.[38] In solid state and in solution compound **19-al** exists as an aldehyde (*vide infra*). Its content in post-reaction mixtures was up to 20%. Relatively large amounts of **19-al** were found in reactions carried out in toluene and DMF.

21-*o′*-OH and 19-al: structures in solid state and in solution

21-*o′*-OH

The structure of compound **21-*o′*-OH** in the solid state was finally confirmed by X-ray structure analysis. Details characterizing the X-ray structure of **21-*o′*-OH** are included in Tables S1-S5. Compound **21-*o′*-OH** crystallizes in the non-centrosymmetric space group *Pc* with one molecule in the asymmetric unit. The oxytetraethylenoxy chain is attached to phenyl rings of azobenzene in the *ortho* and *para′* location in relation to the azo group. A view of the molecule with intramolecular hydrogen bonding is shown in Figure 2. Selected bond lengths [Å] and angles [°] in the crystal structure of **21-*o′*-OH** are: N1-N2 1.273(3), C1-N1 1.403(3), C20-N2 1.412(3), C2-O6 1.344(3), C1-N1-N2 113.8(2), N1-N2-C20 116.6(2), C1-C2-O6 122.0(2).

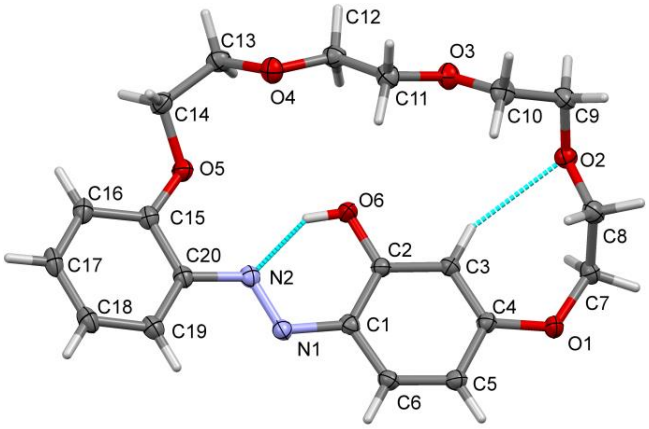

Figure 2. Molecular view of **21-*o′*-OH** with atom numbering scheme and selected hydrogen bonds. Displacement ellipsoids drawn at 50% probability level.

One relatively strong internal hydrogen bond of the O-H···N type is formed between the hydroxyl group (O6-H6) and the N2 atom from the azo group. Another weak C-H···O hydrogen bonding (C3-H3…O2) may play some role in stabilization of the molecular conformation (Table S2). Main intermolecular interactions include stacking of rings C1-C6 and C15-C20 (x,1-y,1/2 +z) and weak C-H···O hydrogen bonding. Crystal packing showing intermolecular interactions is shown in Figure S8.

19-al

The structure of **19-al** (Figure 3) was also determined by the X-ray method. Crystal data and structure refinement for **19-al** are included in Tables S6-S10. **19-al** forms red crystals satisfying symmetry of the monoclinic system, the space group *Ia* (no. 9, unique axis b, cell choice 3 of *Cc*). The asymmetric unit contains one molecule and the whole unit cell is built from four molecules, Z = 4. Most of the bond lengths and angles are in the expected ranges, especially in the etheric part. Based on short interatomic distances one may assume the mostly double character of N2-C19, C15-C16 and C17-C18 bonds. The short C20-O6 bond length confirms its aldehyde character, which is also observed in NMR spectra. Selected bond lengths (Å) and angles (°) in the crystal structure of **19-al** are: N1-N2 1.219 (10), N1-C1 1.450 (13), N2-C19 1.290 (9), C20-O6 1.221 (8), C15-C16 1.376 (12), C16-C17 1.465 (12), C17-C18 1.341 (12), C18-C19 1.501 (10), C19-C15 1.443 (11), C18-C20 1.444 (11), C1-N1-N2 125.3 (7), N1-N2-C19 120.7 (8), C18-C20-O6 124.1 (7).

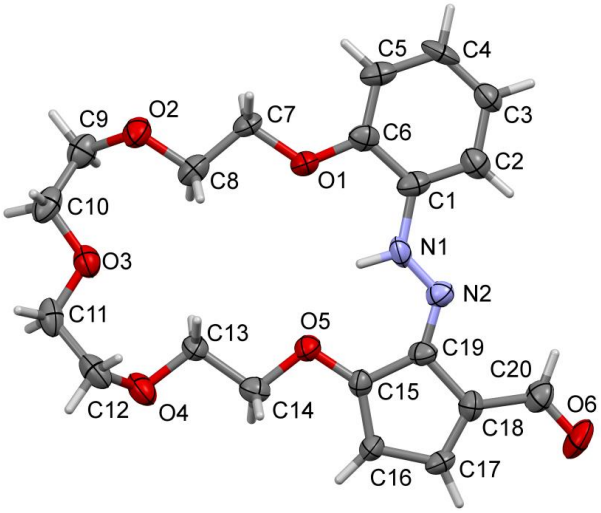

Figure 3. Molecular structure of compound **19-al**, showing the atom labelling scheme. Displacement ellipsoids are shown at 50% probability. Only one (i.e. populated 56.9%) disorder part is presented. The other disorder part forms bonds O1-C15A and O5-C6A (see Figure S10).

Details of the hydrogen bonds are reported in Table S7. The internal N1-H1···O5 (or N1A-H1A···O1 in the second disorder part) hydrogen bond stabilizes the conformation of the molecule, which is essentially flat. Additional weaker CH···O intermolecular interactions form layers of the molecules in the crystalline state parallel to the crystallographic (101) plane (Figure S9). The network of hydrogen bonding for **19-al** is shown in Figure 4.

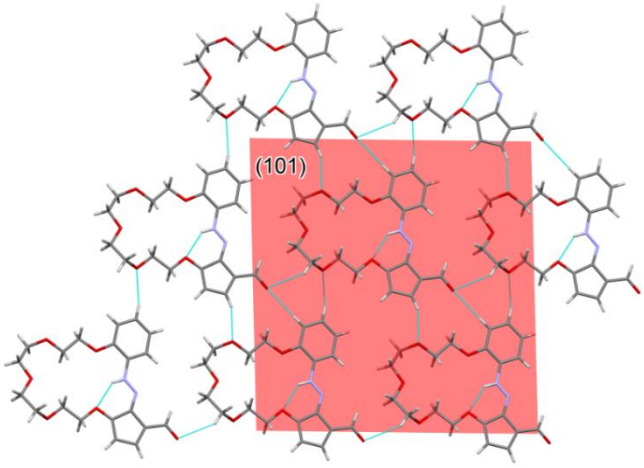

Figure 4. 19-al. Network of hydrogen bonding within the layer parallel to (101). Internal NH…O hydrogen bonds and intermolecular CH…O interactions can be readily noticed. For details see Table S10. The second disorder part omitted.

For comparison, the structures of **21-*o*′-OH** and **19-al** were studied in solution using NMR spectroscopy. 2D NMR studies, consisting of ROESY, HSQC and HMBC experiments, allowed full proton and carbon assignments of **21-*o*′-OH** and **19-al** compounds

(see Supporting Information). ROESY experiments were applied to determine their conformation in solution. These results for **21-*o*'-OH** revealed a close proximity between the aromatic moiety of the 2-position OH-6 residue and the aromatic proton H-3 with the methylene groups of the crown ether chain, positioning the hydroxyl group within the ring of the tested compound. The main ROE correlations are presented in the corresponding structure in the Figure 5. Thus, the DMSO solution conformation of **21-*o*'-OH** appears to be similar to that observed in the crystalline state.

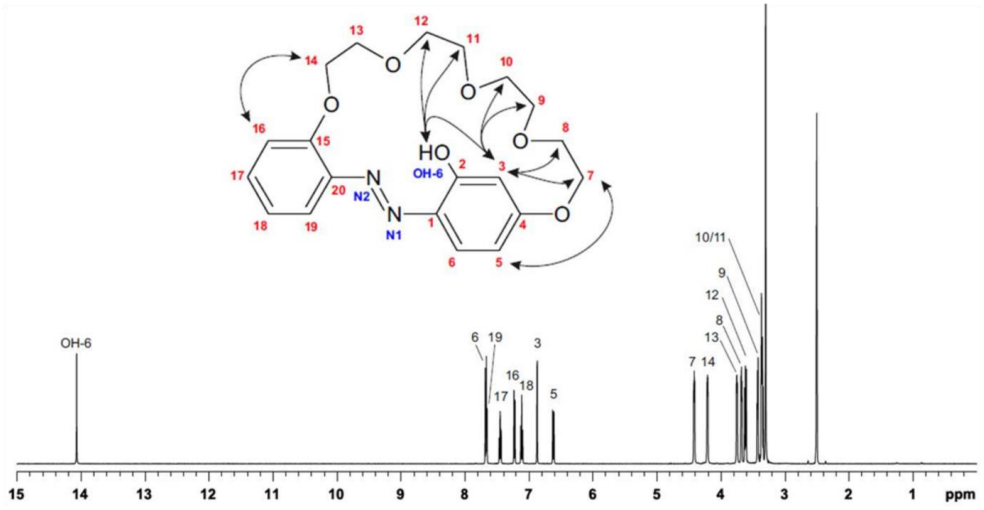

Figure 5. ^{1}H NMR ([D6]DMSO) spectrum of **21-*o*'-OH** with labeling signals of individual protons and with main ROE correlations shown.

19-al in solution ([D6]DMSO) exists in two forms: *Z* and *E*. Only one of them, *Z* was found in the crystalline solid state. The double bond between C-19/N-2 corresponds to major *E* and minor Z geometry isomers (Figure 6 and Supporting Information). The double bond at C-19 was assigned with *E*-geometry as a result of the observation of ROEs: H-N1/H-20 and H-N1/H-2. The *Z*-configuration of C-19 in the molecule was confirmed by the fact that no ROEs between H-N2 were detected to H-2 and H-20, but instead, only ROEs between H-N1 and the nearest methylene groups of the crown ether chain H-7, H-8, H13, H-14 were clearly observed. While the *Z*-geometry presents a planar conformation analogous to the crystalline state, the anisotropic shielding effect of the aromatic ring on H-9, H-10, H-11 and H-12 determines a rather folded conformation, where the aromatic ring is perpendicularly orientated in relation to the whole ether crown molecule ring (see Dreiding models, Figure S4.mod). Protons at 11.14 and 13.92 ppm in ^{1}H NMR spectra are exchangeable with D_2O.

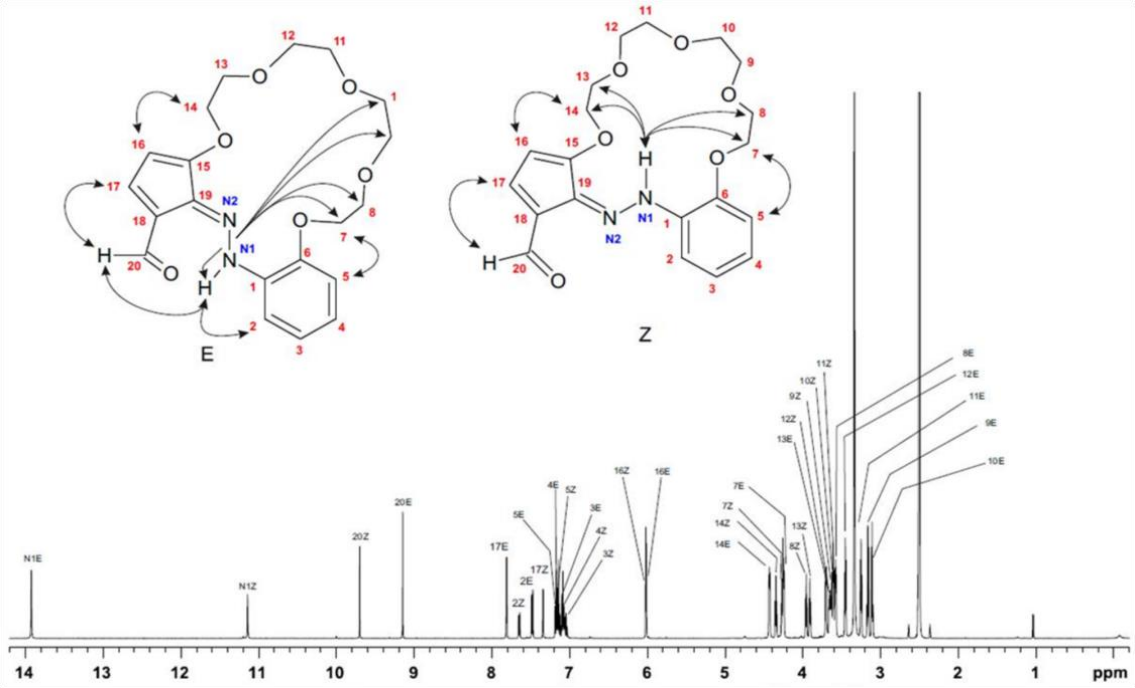

Figure 6. [1]H NMR ([D6]DMSO) spectrum of **19-al** with labeling signals of individual protons attributed to two isomers *E* and *Z* and with shown main ROE correlations (see Figure S4a).

Tautomeric equilibrium

Analyzing the tautomeric azophenol⇄quinone-hydrazone equilibrium of macrocyclic hydroxyazocompounds (Scheme 5) apart from location of substituent(s), type of solvent, pH and ionic environment[13] the size of the macrocycle should be also taken into consideration.[7-12]

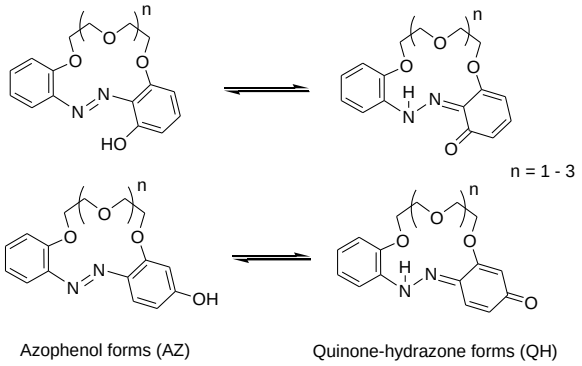

Scheme 5. Scheme of the tautomeric equilibrium of hydroxyazobenzocrowns.[7-12].

Our previous studies[10,11,40] have shown that 13- and 16-membered *p*-hydroxyazobenzocrowns can exist in two tautomeric forms: quinone-hydrazone (QH) and azophenol (AZ). The tautomeric equilibrium was found to be strongly dependent on the size of the macrocycle and the type of solvent. 13- and 16-membered crowns in most solvents exist predominantly in quinone-hydrazone forms. Azophenol tautomers were detected among others in DMSO. The existence of tautomeric equilibrium for 19-membered *p*-hydroxyazobenzocrown **19-*p*-OH** was signalized earlier,[7] but it was not studied in detail.

The solvent effect on tautomeric equilibrium of **19-*p*-OH** can be observed both in UV-Vis absorption and in emission spectra (Figure 7). The absorption band characteristic for the quinone-hydrazone (QH) form is observed at ~ 440 nm, azophenol (AZ) absorbs at a lower wavelength ~ 345 nm (Figure 7a). The position of maxima of absorption bands and the value of the molar absorption coefficient are dependent on the type of solvent (Table S11). The emission peak of quinone-hydrazone of **19-*p*-OH** is located at ~ 540 nm (Figure 7b).

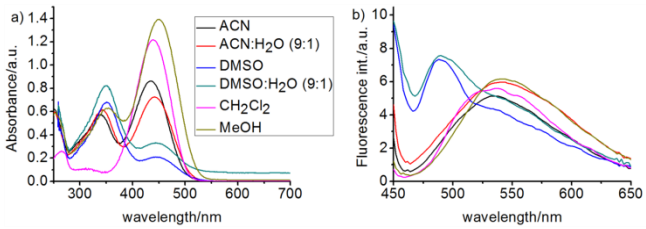

Figure 7. Comparison of bands of a) UV-Vis absorption (line corresponding to the DMSO:water mixture. A value over zero suggests precipitation of the crown in this mixture of solvents) and b) emission spectra of **19-*p*-OH** (5.6×10^{-5} M) in different solvents. ACN=acetonitrile.

On the basis of UV-Vis absorption spectra of **19-*p*-OH** (concentration ~10^{-5} M) it can be concluded that only in the relatively non-polar, aprotic (non-hydrogen bond donor) dichloromethane the QH form is predominant (93%). The distribution of QH changes with the type of solvent: methanol (69%), acetonitrile (60%) and the mixture of the last with water (55%). In DMSO - an aprotic, highly dipolar and hydrogen bond acceptor solvent of relatively high basicity, the main absorption band is found at 351 nm, corresponding to the azophenol tautomer (76%). It was reported that in DMSO azophenol tautomers are observed in their anionic form.[39] This finds confirmation in emission spectra registered for the diluted solution, where only in DMSO and its mixture with water the emission band is found at 488 nm. It can be attributed to the anionic form of the azophenol tautomer (Figure 7b). At this point one more factor is worth noting, influencing the distribution ratio of tautomers of **19-*p*-OH**, namely concentration. It was concluded that the distribution of individual forms

depends on the total concentration of crown. In acetonitrile the percentage of azophenol increases with the increase of the total concentration of crown (Figure 8a).

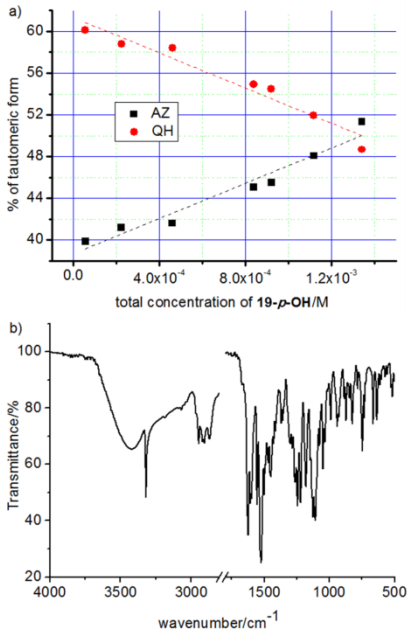

Figure 8. a) The trend (UV-Vis absorption spectra) of distribution of tautomers of **19-*p*-OH** as a function of total concentration of crown in acetonitrile b) infrared spectrum of **19-*p*-OH** (KBr pellet)

The contribution of individual tautomers of **19-*p*-OH** under equilibrium in solvents of different nature was also estimated on the basis of ^{1}H NMR spectra (Table 1) at crown concentration ~10^{-2} M. Examples of ^{1}H NMR spectra and ^{13}C NMR spectrum of **19-*p*-OH** are shown in Figures S1a-c. Opposite to crowns of smaller macroring size, tautomeric equilibrium of **19-*p*-OH** is shifted towards the azophenol form, with its strong predominance in DMSO.

Table 1. Quantitative contribution of tautomers in quinone-hydrazone (QH)⇄azophenol (AZ) equilibrium of *p*-hydroxyazobenzocrowns (at ~10^{-2} M) in different solvents (on the basis of ^{1}H NMR)

	Acetonitrile	**Acetone**	**Chloroform**	**DMSO**
13-*p*-OH [7-12]	QH	QH	QH	70% QH; 30% AZ
16-*p*-OH [7-12]	QH	QH	QH	AZ
19-*p*-OH	25% QH; 75% AZ	45% QH; 55% AZ	40% QH; 60% AZ	AZ

It was confirmed by the analysis of X-ray structures of 13- and 16-membered crowns that in the solid state these compounds exist in quinone-hydrazone forms.[12,40,41] For **19-*p*-OH** attempts to obtain crystals suitable for X-ray analysis failed, thus the presence of the quinone-hydrazone form in the solid state can be to a high extent confirmed by the infrared spectrum

(Figure 8b): a strong and sharp band at 3320 cm^{-1} corresponding to νN-H vibrations and the carbonyl group νC=O signal at 1625 cm^{-1}.

Compounds **19-*o*-OH** and **21-*o′*-OH** in solution exist in azophenol forms with main absorption bands located at 363 and 395 nm, respectively (acetonitrile). The type of solvent has no spectacular influence on their spectral properties, namely the position of the absorption maximum. The position of absorption bands and the values of molar absorption coefficients are collected in Table S12. Both compounds **19-*o*-OH** and **21-*o′*-OH** are hardly fluorescent. NMR spectra of compounds **19-*o*-OH** and **21-*o′*-OH** registered in different solvents are shown in Figures S2-S3.

Acid-base properties vs. tautomeric equilibrium

Simple azocompounds behave as weak bases. On the other hand the presence of the hydroxyl group introduces a weak acid moiety into the azobenzocrown skeleton. Moreover, the protonation/deprotonation of macrocylic *p*-hydroxyazobenzocrowns can influence the change of tautomeric equilibrium.

Acid-base properties of 19- and 21-membered hydroxyazobenzocrowns were investigated by UV-Vis absorption and emission spectrometries in acetonitrile. Upon titration of solutions of crowns with *p*-toluenesulfonic acid, as could be expected, a new band of a large bathochromic shift (over 100 nm) - corresponding to protonated azophenol forms (Scheme S1) - for all macrocyles investigated here is observed. This is connected with a significant color change from yellow/orange to red. Well pronounced isosbestic points suggest one system under equilibrium (Figure 9).

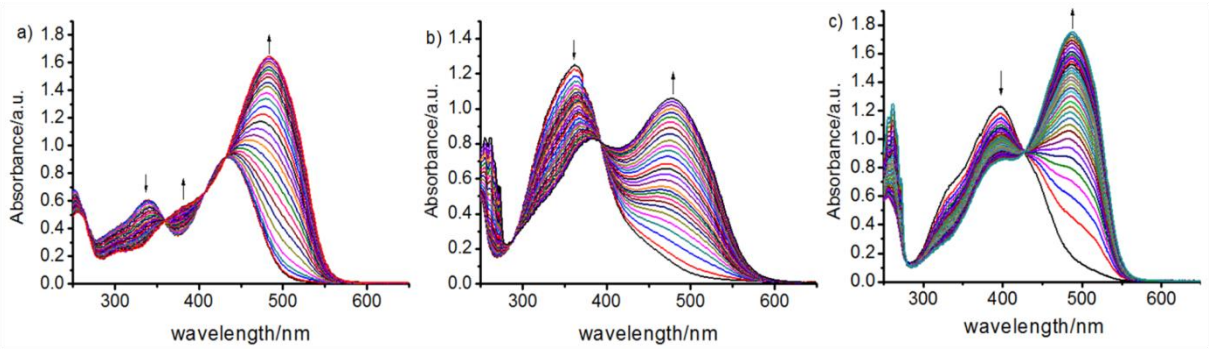

Figure 9. Changes in UV-Vis absorption spectra of hydroxyazobenzocrowns upon titration with *p*-toluenesulfonic acid (TosOH): a) **19-*p*-OH:** $c_{crown}=5.6\times10^{-5}$ M; $c_{TosOH}=0\text{-}9.1\times10^{-5}$ M b) **19-*o*-OH:** $c_{crown}=7.6\times10^{-5}$ M; $c_{TosOH}=0\text{-}1.1\times10^{-3}$ M c) **21-*o′*-OH:** $c_{crown}=7.37\times10^{-5}$ M; $c_{TosOH}=0\text{-}1.4\times10^{-3}$ M in acetonitrile.

The comparison of proton binding constants obtained from UV-Vis absorption titration shows the trend for *p*- and *o*-hydroxyazobenzocrowns of different size of macrocyle. The protonation constants are higher for *p*-isomers (Scheme S1) and the larger the macrocycle the smaller the proton affinity ($\log K_a$). The determined proton binding constant $\log K_a$ 3.50±0.03 for compound **21-*o′*-OH** is comparable to the value found for the 19-membered *o*-hydroxyazobenzocrown.

Protonated forms of 19- and 21-membered hydroxyazobenzocrowns studied here are fluorescent. The change of emission spectra upon titration with a solution of *p*-toluenesulfonic acid in acetonitrile is shown in Figure S11.

The average proton binding constant values ($\log K_a$), calculated from two independent fluorescence measurements, for investigated macrocycles are 4.08±0.05, 3.50±0.25 and 4.14±0.06 for **19-*p*-OH, 19-*o*-OH** and **21-*o′*-OH**, respectively. The obtained values are, in general, comparable with constants from UV-Vis measurements. A difference was found for the 21-membered compound for which the protonation constant obtained from absorption measurements is significantly lower.

Titration of 19- and 21-membered crowns with a solution of *tetra*-n-butylammonium hydroxide (TBAOH) in acetonitrile results in noticeable changes in UV-Vis absorption spectra (Figure 10a-c) connected with well observable color changes from yellow to purple. It is best pronounced for **19-*o*-OH** as a consequence of the largest bathochromic shift ($\Delta\lambda$ =150 nm) of the absorption band between azophenol and its ionized form. This is a similar trend as for the spectral behavior in the presence of acid. Spectral changes upon ionization are more significant for azophenol forms of hydroxyazocompounds than for the quinone-hydrazone tautomer. The comparison of the absorption band shift between ionized and non-ionized forms of compounds studied here is shown in Figure 10d.

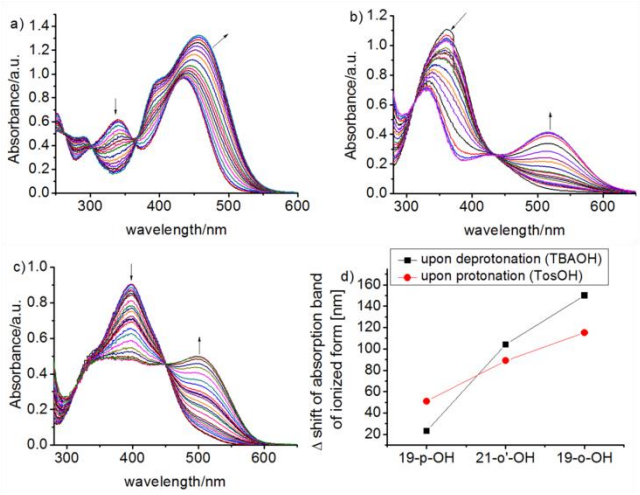

Figure 10. Changes in UV-Vis absorption spectra upon titration of hydroxyazobenzocrowns with tetra-n-butylammonium hydroxide a) **19-*p*-OH** (c_{crown}=5.6×10^{-5} M; c_{TBAOH}=0-1.9×10^{-4} M) b) **19-*o*-OH** (c=7.9×10^{-5} M; c_{TBAOH}=0-1.8×10^{-3} M) c) **21-*o′*-OH** (c=8.1×10^{-5} M; c_{TBAOH}=0-2.0×10^{-3} M) d) the comparison of the difference in the position of absorption bands [nm] between ionized and non-ionized forms of compounds **19-*p*-OH, 19-*o*-OH** and **21-*o′*-OH** in acetonitrile.

In emission spectra of **19-*p*-OH** registered in the presence of TBAOH at the beginning fluorescence quenching is observed (Figure S12a) until an equimolar ratio crown to base (pink line) is reached. Increase of the base concentration changes the titration trace to a blue shift (30 nm) of the emission band and next an increase of fluorescence intensity is observed. A new emission band at ~500 nm corresponds to the deprotonated azophenol form of **19-*p*-OH**. The molar ratio plot with a minimum at a value close to 1 (Figure S12b) suggests that changes in emission spectra can correspond to the gradual formation of deprotonated azophenol form. The equilibrium constant logK_b derived from fluorescence measurements logK_b 3.98±0.11 is close to the value obtained from UV-Vis absorption spectra estimated as logK_b 3.68±0.08 and can be treated as a measure of dissociation of **19-*p*-OH**. For comparison, literature data of the dissociation constant for a crown ether with peripheral azo group with a hydroxyl residue in the *para* position was found to be logK_b 3.95 (55% dioxane in water).[42] The change of tautomeric equilibrium upon ionization in acidic (*p*-toluenesulfonic acid) and basic (*tetra*-n-butylammonium hydroxide) media also finds confirmation in ^{1}H NMR spectra of **19-*p*-OH** (45% QH, 55% AZ, [D6]acetone) (Figure S13). The most characteristic signal for quinone-hydrazone at 5.93 ppm is not observed in acidic, as well as basic solution, this being connected with the spectral pattern of signals attributed to C_{ar}-H protons pointing to the existence of the protonated/deionized azophenol form in solution.

Metal cation complexation

Alkali and alkaline earth metal cation complexation by 19-membered and 21-membered hydroxyazobenzocrowns was investigated using mainly UV-Vis absorption and emission spectroscopies in acetonitrile. For comparison with the results obtained previously for hydroxyazobenzocrowns of smaller macrorings, the effect of the presence of triethylamine and additionally TBAOH on the character of spectral changes induced by metal salts was also investigated. It was found that the presence of metal salts does not cause significant changes in absorption and emission spectra in a water containing system (acetonitrile:water, 10:1).

19-*p*-OH

For **19-*p*-OH** the spectral response in UV-Vis absorption spectra, in acetonitrile, was observed in the presence of lithium, sodium, potassium and magnesium, calcium, strontium and barium perchlorates. The general trend of changes (Figure S14) upon spectrophotometric titration is the decrease of the absorption band at ~430 nm and the increase of the intensity of the band at ~340 nm. These changes can correspond to the change of tautomeric equilibrium upon metal cation complexation, namely its shift towards the azophenol form. It is a similar spectral behavior to the earlier studied 16-membered macrocycles.[12] Noteworthy, spectral changes (Figure S14c) in the presence of the magnesium salt are slightly different. It is the only case, when the absorption band of the complex band is red shifted. A relatively slight bathochromic shift in neutral acetonitrile and the existence of a band at ~340 nm in the UV-Vis spectrum can suggest that the non-ionized azophenol form is present with a coexisting quinone-hydrazone tautomer under equilibrium.

In pure acetonitrile the highest stability constant (logK) value was found for sodium among alkali metal cations and for the calcium salt among alkaline earth metal complexes - ions of similar ionic radius. The comparison of logK for **19-*p*-OH** and the reference 19-membered azobenzocrown **19AZB**[6] is shown in Figure 11 and collected in Table S13. For the 19-membered *p*-hydroxyazobenzocrown stability constant values of complexes with sodium and potassium salts are higher than for the parent **19AZB**.

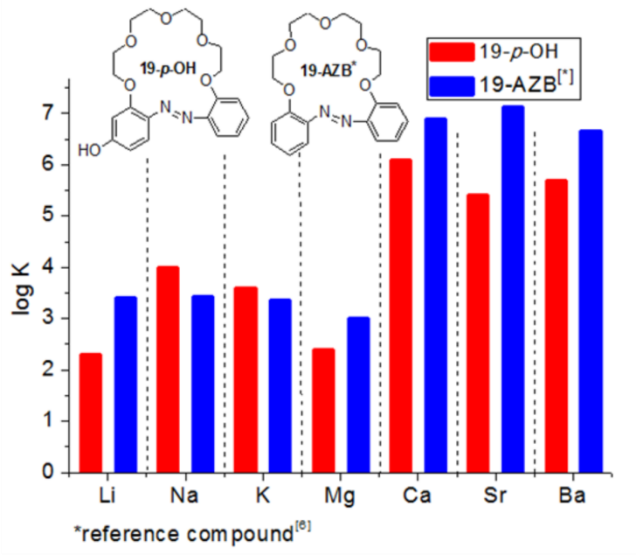

Figure 11. The comparison of stability constants values of complexes of **19-*p*-OH** and **19AZB** in acetonitrile

^{1}H NMR spectra of **19-*p*-OH** ([D6]acetone) registered in the presence of equimolar crown to metal perchlorate amounts are shown in Figure S15. In the case of the lithium salt the presence of two tautomers under equilibrium is observed with a slightly shielded signal of the O-H proton ($\Delta\delta$ = 0.14 ppm) coming along with a slight rearrangement of the aromatic proton signal pattern. The sodium complex is formed by the azophenol form. The same mode of cation binding can be assumed for potassium and alkali earth metal cations, besides magnesium. The ^{1}H NMR spectrum of the magnesium complex registered in [D6]acetone shows distorted signals of all protons (thus signals in the spectrum of the complex cannot be easily ascribed to a particular proton). This can be connected with fast exchange processes and/or coordination by two tautomers in solution. The FTIR spectrum (KBr pellet) of **19-*p*-OH** complex with magnesium perchlorate (Figure S16) presents a broad band in the region of νC=O of the quinone-hydrazone group vibration (~1620 cm^{-1}) (in the complex overlapping with the νC=C band) compared to the FTIR spectrum of the uncomplexed macrocyle.

Fluorescent properties of the quinone-hydrazone form of earlier studied *p*-hydroxyazobenzocrowns[12] have prompted us to study the effect of the presence of metal salts on tautomeric equilibrium of **19-*p*-OH** traced by emission spectra. For **19-*p*-OH** in most cases the decrease of the fluorescence intensity is observed. Changes in emission spectra of **19-*p*-OH** registered upon titration with metal perchlorates in pure acetonitrile are exemplified in Figure 12. The degree of quenching is dependent on metal perchlorate and can be illustrated by estimated values of the Stern-Volmer constant (log K_{SV}). The analysis of Stern-

Volmer plots suggests that fluorescence quenching for **19-*p*-OH** by metal perchlorates cannot be treated as a pure dynamic or pure static process. Only in the case of lithium and to some extent potassium the Stern-Volmer plots are linear, for sodium down-curved and for all alkaline earth metal cation salts up-curved (Figure S17). The modified Stern-Volmer equation[43,44] seems not to be applicable to the case of **19-*p*-OH** - no reasonable straight line was obtained. Thus, it can be assumed, also on the basis of ^{1}H NMR and UV-Vis absorption titration experiments described above, that the deviation of linearity for the Stern-Volmer equation can be explained by the more complex nature of fluorescence quenching: both collisional, static and a strong influence of the change of tautomeric equilibrium upon metal cation complexation[45] also in excited state. However, saying that, K_{sv} (Figure 12c) have been estimated (Table S14) taking the linear range of plots to show the relationship between the type of metal cation and the fluorescence quenching ability. Sodium (among alkali metal cations) and calcium (among alkaline earth metal cations) salts have the strongest effect on fluorescence quenching. The tendency can be put in the order: Na>K>Li and Ca>Sr~Ba, being close to the order of stability constant values of complexes determined from UV-Vis absorption spectra.

Stability constants values (Table S13) for complexes of **19-*p*-OH** estimated from fluorescence experiments for alkali metal cation complexes, even though correlating with values obtained from UV-Vis measurements, must be treated as approximate ones. For the magnesium complex, logK was estimated as <2.

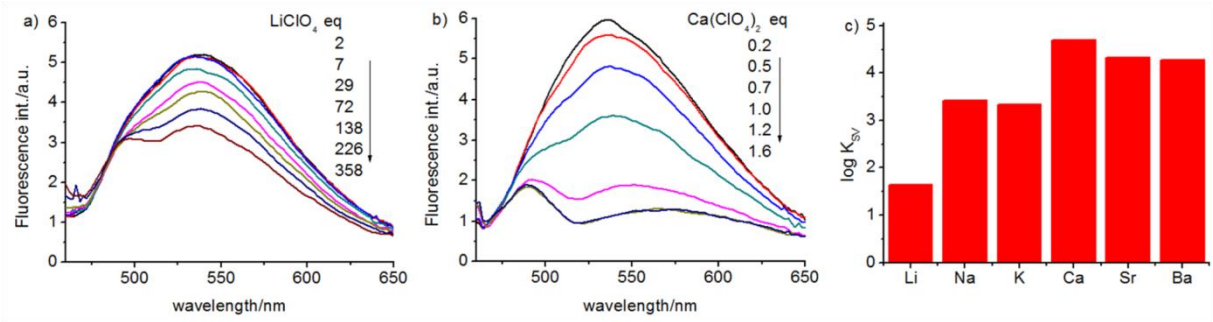

Figure 12. Changes in emission spectra of **19-*p*-OH** (λ_{ex}=434 nm, λ_{em}=536 nm) upon titration with a) lithium ($c_{crown}=3.4\times10^{-5}$ M) b) calcium ($c_{crown}=5.8\times10^{-5}$ M) c) the fluorescence quenching trend by metal perchlorates for **19-*p*-OH**, based on estimated Stern-Volmer constant ($logK_{SV}$) values in acetonitrile.

Previous research[12] showed that hydroxyazobenzocrowns may form complexes with metal perchlorates as ionized quinone-hydrazone tautomers in acetonitrile with addition of

triethylamine (TEA). A similar behavior was also found for **19-*p*-OH**. Changes are more significant than in case of the 16-membered analog dependent on the type of metal perchlorate. In the presence of triethylamine only titration with lithium salt, opposite to sodium and potassium perchlorates, gives a significant bathochromic shift (~30 nm) of the complex spectral band (Figure S18a). However, it was noticed that after addition to the solution of **19-*p*-OH** in basic acetonitrile (130-fold excess of Et_3N), the titration trace for the lithium salt changes within the experiment duration (Figure S18b). Within 20 minutes after addition of the salt the system returns back to the uncomplexed form. Thus, the stability constant with lithium perchlorate under such measurement conditions can be given only as an estimated value: log K ~3. For the sodium salt in the presence of triethylamine (13-fold excess) the main changes in absorption spectra are manifested by the increase of intensity of the band characteristic for the azophenol form (~350 nm). At a higher concentration of TEA spectral changes with the appearance of a red shifted absorption band at ~ 450 nm are observed (Figure S19a). A comparable spectral trace is obtained when the solution of **19-*p*-OH** is titrated with sodium perchlorate in the presence of 130 eq. of TEA. Analysis of the ^{1}H NMR spectrum of the sodium complex registered in the presence of the excess of triethylamine (Figure S20) indicates that sodium in basic solution forms complexes with the ionized azophenol tautomer of **19-*p*-OH**. By analogy, a similar conclusion can be drawn from the titration experiment with the potassium salt, however the bathochromic shift in UV-Vis absorption spectra is less significant than in the case of the sodium experiment (+6 and +8 nm for bands 340 and 435 of crown). Stability constants of 1:1 complexes of **19-*p*-OH** with sodium and potassium perchlorates calculated from titration experiments are logK 4.2±0.4 and 3.8±0.1, respectively. For calcium, strontium and barium perchlorates in acetonitrile (the presence of 130-fold excess of Et_3N) a similar trend in UV-Vis absorption spectra changes, i.e. the bathochromic shift of both bands at ~350 and ~435 nm is observed. The titration trace for alkaline earth metal perchlorates is illustrated by the changes of spectra in the presence of barium perchlorate in Figure 13a. Opposite to sodium and potassium a more significant increase of band intensity at longer wavelengths is observed. The value of the red shift can be correlated with the type of metal cation and increases in the order: Ba>Sr>Ca. This trend seems to reflect the tendency of cations for shifting of equilibrium towards ionized azophenol of the same order for as stability constant values (log K): Ba>Sr>Ca (Figure 13b). Similarly to lithium, also for experiments with alkaline earth metal cations the change of absorption within the timescale was observed (the most significant for strontium), thus stability constant values should be treated as estimative.

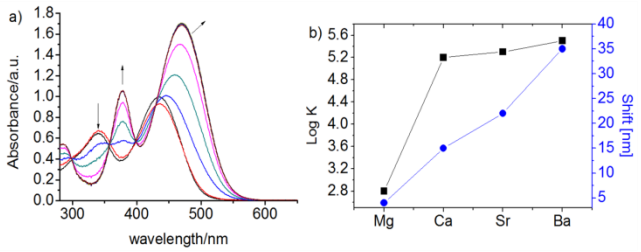

Figure 13. a) Changes in the UV-Vis spectrum of **19-*p*-OH** (c_{crown}=5.83×10^{-5} M) upon titration with barium perchlorate (c_{salt}= 0–1.2×10^{-4} M) in acetonitrile (130-fold excess of Et_3N) b) the comparison of stability constant values logK of (1:1) complexes of **19-*p*-OH** (black squares) with alkaline earth metal salts and the spectral shift [nm] of absorption band ~ 450 nm in UV-Vis spectra for the complexes.

In the case of the magnesium salt the trend of spectral changes in UV-Vis absorption spectra is more dependent on the salt concentration than it is for the rest of investigated alkaline earth metal perchlorates (Figure S21). More excess of the magnesium salt gives spectral changes within the long wave absorption region (~450 nm).

Metal cation complexation and tautomeric equilibrium of **19-*p*-OH** was also investigated in the presence of a stronger than triethylamine, organic base, namely *tetra*-n-butylammonium hydroxide (TBAOH). In the presence of 10-fold excess of TBAOH (larger amounts give spectral changes pointing to crown deprotonation) the titration trace with metal perchlorates, in most cases, is similar to the pattern observed for calcium perchlorate, as shown in Figure 14a. The increase of the absorption band characteristic for the azophenol form (~340 nm) and the decrease of the band ascribed to the quinone-hydrazone tautomer (~435 nm) with none or a negligible spectral shift is observed. Again, as it was shown above, the magnesium and lithium perchlorates titration trace gives different results, as is exemplified by the magnesium titration trace in Figure 14b. Magnesium perchlorate in the presence of TBAOH seems to shift the tautomeric equilibrium towards the quinone-hydrazone form. The values of stability constant logK of 1:1 complexes of **19-*p*-OH** with metal perchlorates in basic (TBAOH) acetonitrile are shown in Figure 14c. The increase of binding constant values is well observed according to metal ion size, only strontium is out of this trend. For the last case some other than simple host-guest size complementarity must influence the stability constant value.

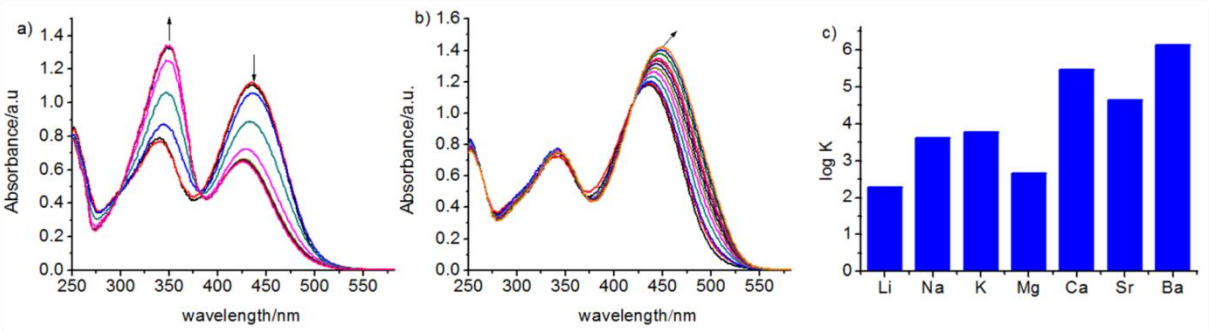

Figure 14. Changes in the UV-Vis spectrum of **19-*p*-OH** in basic acetonitrile (10-fold excess of TBAOH) upon titration with: a) calcium (c_{crown}=5.8×10^{-5} M, c_{salt} = 0-3.6×10^{-4}) b) magnesium (c_{crown}=5.8×10^{-5} M, c_{salt}=0-3.5×10^{-3} M) c) the values of the stability constant logK of 1:1 complexes of **19-*p*-OH** with metal perchlorates in basic (TBAOH) acetonitrile.

19-*o*-OH

Metal cation complexation for **19-*o*-OH** was studied in an analogous way to the 19-membered *p*-substituted analog presented above. Spectral data (^{1}H NMR) show that in acetonitrile solution only one tautomer, namely the azophenol form, is present. In neutral acetonitrile spectral changes in UV-Vis absorption spectra were observed for all investigated metal perchlorates. Complex formation is manifested by increase of the band intensity at ~450 nm and the hypsochromic shift of the absorption band positioned at 363 nm for the uncomplexed crown. The presence of alkaline earth metal cations: calcium, strontium and barium (Figure15a) causes more significant spectral changes than alkali metal cations and the magnesium salt.

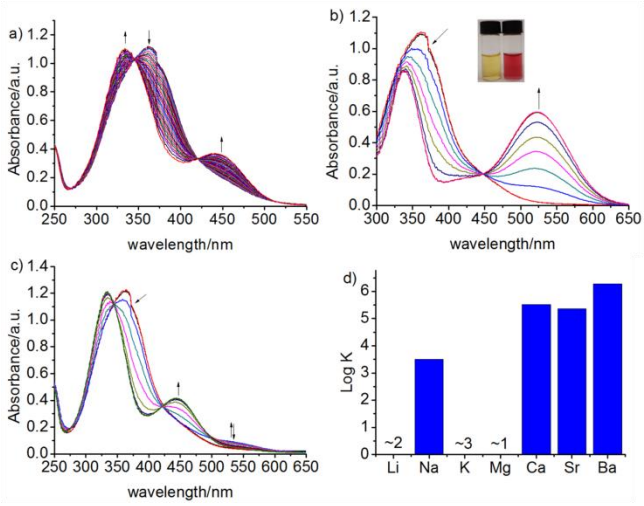

Figure15. Changes in UV-Vis absorption spectra of **19-*o*-OH** upon titration with barium perchlorate a) (c_{crown}=7.7×10^{-5} M, c_{salt}=0-1.3×10^{-4} M) in acetonitrile b) (c_{crown}=7.7×10^{-5} M, c_{salt}=0-1.3×10^{-4} M) in the presence of 130-fold excess of triethylamine and the color change of the crown solution in the presence of excess of barium salt in basic (Et_3N) acetonitrile c) (c_{crown}=7.9×10^{-5} M, c_{salt}=0-1.2×10^{-4} M) in basic acetonitrile (3-fold molar excess of TBAOH) d) the values of stability constant of 1:1 complexes of **19-*o*-OH** with metal perchlorates in neutral acetonitrile.

The stability constant values (logK) for 1:1 complexes of **19-*o*-OH** calculated from UV-Vis titration experiments are shown in Figure 15d and collected in Table S13. For alkali metal salts only in the case of the sodium complex changes allowed to calculate a reliable value of the stability constant. The highest value of binding constant among all investigated metal salts was found for the barium complex, logK 6.27±0.08.

The ^{1}H NMR spectrum of **19-*o*-OH** in [D6]acetone (Figure 16) is characterized by relatively high position of the O-H proton signal: 14.05 ppm. For comparison, this signal in spectra of **13-*o*-OH** and **16-*o*-OH** is observed at 12.7 and 13.4 ppm, respectively.[11] It can indicate, that in the case of *ortho*-hydroxyazobenzocrowns the strength of the intramolecular hydrogen bond increases with increase of the macrocycle size. A longer, more flexible polyether chain may influence the geometry of the molecule enabling the formation of more effective O-H···N=N-hydrogen bonding. Metal cation complexation occurs mainly with engagement of middle one oxygen atoms of the polyether moiety and probably one of the nitrogen atoms of the azo residue (by analogy to the described structure of the sodium complex of the 16-membered azobenzocrown, cf.[46]) As can be expected complex formation changes the geometry of the host molecule, also probably weakening the intramolecular hydrogen bond. This is well supported by the ^{1}H NMR spectrum of **19-*o*-OH** registered in the presence of two-fold excess of sodium perchlorate ([D6]acetone) (Figure 16). In the complex, besides

the changes within signals of polyether and aromatic protons, shielding of the OH proton is observed ($\Delta\delta$ = -1.9 ppm)

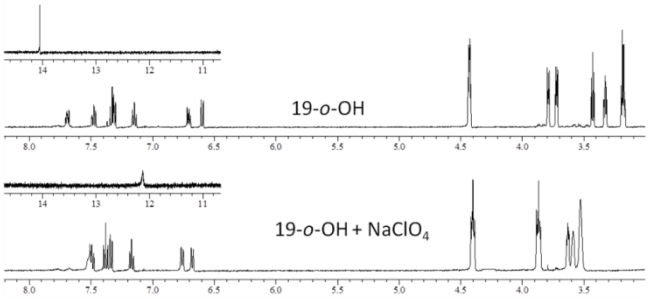

Figure 16. ^{1}H NMR spectrum of **19-*o*-OH** (c= 1.4×10^{-3} M) and its comparison with the spectrum registered in the presence of two-fold excess of sodium perchlorate ([D6]acetone).

In the presence of triethylamine more significant than in neutral acetonitrile, i.e. larger, bathochromic shifts of the complex band are observed for calcium ($\Delta\lambda$ = +71 nm), strontium ($\Delta\lambda$ = +75 nm) and barium ($\Delta\lambda$ = +80 nm) titrations, resulting in color changes from yellow to purple. Alkali metal perchlorates give small, but observable spectral changes. In the case of the magnesium salt the effect of salt presence can be treated as negligible. Unfortunately, all systems in which triethylamine was used as a base, were found to be more or less unstable under measurement conditions. Exceptions are sodium and potassium titrations for which changes within the experiment timescale of were less noticeable, but too small to calculate reliable values of stability constants. Estimates of stability constant values logK are collected in Table S13.

Titration of **19-*o*-OH** with metal perchlorates in the presence of *tetra*-n-butylammonium hydroxide (3-fold molar excess to crown, a larger amount gives spectral changes pointing to deprotonation of hydroxyazobenzocrown) results in noteworthy, but less significant and slightly different changes than observed in experiments where triethylamine was used. The titration trace under these conditions is illustrated by a spectral trace obtained for barium perchlorate in Figure 15c. The highest value of stability constants was found for calcium perchlorate, whereas complexes with strontium and barium are characterized by comparable binding constants (Table S13).

21-*o*′-OH

UV-Vis absorption spectra of **21-*o*′-OH** in pure acetonitrile are significantly affected only by the presence of magnesium, calcium and strontium perchlorates. The most interesting and selective spectral response was found for magnesium perchlorate (Figure 17a) - also

observable as a color change from yellow to orange (Figure 17a). The relationship $\Delta A=f(\log c_{Mg\ salt})$, where ΔA is the difference between the absorbance value at a given concentration of magnesium salt and absorbance observed for the "free" crown at a given wavelength (inset Figure 17a) is linear. However, the weak point of magnesium selective recognition by **21-*o*′-OH** in acetonitrile is the overlapping of the band of its complex with calcium and strontium complex bands. Titration with strontium perchlorate is shown in Figure 17b.

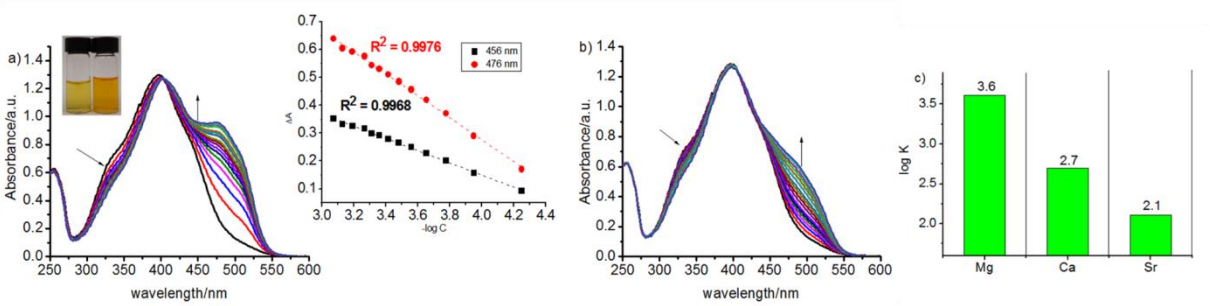

Figure 17. Changes in UV-Vis absorption spectra of **21-*o*′-OH** upon titration with: a) magnesium (c_{crown} = 6.5×10^{-5} M; c_{salt} = 0-1.5×10^{-3} M) and the color change of crown solution in the presence of magnesium perchlorate. Inset: the relationship $\Delta A=f(\log c_{Mg\ salt})$ and b) strontium (c_{crown}=6.5×10^{-5} M; c_{salt}=0-1.1×10^{-2} M) perchlorates c) stability constant values (logK) of 1:1 complexes of **21-*o*′-OH** with alkaline earth metal perchlorates in neutral acetonitrile.

The trend of the obtained stability constant (logK) values (Figure 17c, Table S13) shows a possible relationship between the ion and molecular cavity size: the highest affinity was found for the magnesium cation. The spectral response due to barium perchlorate presence can be regarded as negligible. Magnesium selectivity over calcium and strontium, expressed as the ratio of stability constant values, is 1.3 and 1.6, respectively.

A selective magnesium response was also found for **21-*o*′-OH** in emission spectra as the increase of fluorescence intensity. The stability constant value (logK) 3.79±0.04 of the magnesium complex (1:1) estimated from fluorescence measurements is comparable to the value determined from absorption spectra.

The determination of reliable stability constant values for metal cation complexes of **21-*o*′-OH** in acetonitrile in the presence of triethylamine was not possible due to insignificant spectral changes or changes of absorption spectra within the time scale of the experiment (alkaline earth metal perchlorates). Examples of absorption spectra of **21-*o*′-OH** in basic (Et_3N) acetonitrile registered in the presence of metal perchlorates are shown in Figure S22.

In the presence of a stronger base, *tetra*-n-butylammonium hydroxide, only presence of the magnesium salt gives significant spectral changes - a red shifted complex band of 75 nm (Figure S23). The stability constant value of the 1:1 complex of **21-*o'*-OH** with magnesium perchlorate in acetonitrile in the presence of a crown equimolar amount of TBAOH was estimated as log K≤4.

Conclusions

The photochemical rearrangement of azoxybenzocrowns is an interesting process and seems to be a relatively efficient method of preparation of hydroxyazocompounds. It could be a greener alternative to the classical-chemical Wallach rearrangement, where concentrated acids in the preparation step and a lot of solvents (work-up stage) are used. Moreover, the classical-chemical rearrangement leads mainly to one product: the *p*-hydroxy isomer, whereas in a single photochemical process several products of interesting properties can be obtained. The photochemical procedure allows the synthesis of various hydroxyazocompounds with yields dependent on process conditions. An important novelty is the isolation, besides 19-*ortho* and 19-*para* hydroxyazobenzocrowns, also of a new type of macrocyclic compounds: the 21-membered *ortho*-hydroxyazobenzocrown with *o,p'*-substituted benzene rings **21-o′-OH** and the 19-membered crown bearing an aldehyde moiety, **19-al**. This type of product (to the best of our knowledge) was obtained in such a reaction type for the first time. It was found that the tautomeric equilibrium of 19-membered *p*-hydroxyazobenzocrown **19-*p*-OH** is more complex than has been observed for smaller 13- and 16-membered analogs. Alkali and alkaline earth metal complexes in acetonitrile are formed by the azophenol form of **19-*p*-OH** with the highest stability constant values for sodium and calcium. Metal cation complexation in acetonitrile causes quenching of fluorescence. **19-*o*-OH** in acetonitrile preferentially forms complexes with calcium, sodium and barium among alkaline earth metal cations. A certain sodium affinity, compared to **19-*p*-OH**, over the rest of investigated alkali metal cations is worth noting here. Metal cation complexation in the presence of an organic base (triethylamine, TBAOH) is manifested by a significant bathochromic shift of the complex band and a well observable color change from yellow to purple. The newly obtained 21-membered azobenzocrown with an inherent hydroxyl group **21-o′-OH** shows magnesium selectivity both in neutral and in basic acetonitrile solutions, being well observable in UV-Vis absorption and emission spectra. The properties of the new macrocyle **19-al** are under investigation and will be described elsewhere.

Experimental Section

General considerations

Unless otherwise stated, materials and solvents were of analytical reagent grade obtained from commercial suppliers and were used without further purification. UV-Vis and spectrofluorometric measurements were carried out in commercial solvents of the highest available purity: DMSO (spectroscopic grade, POCh), dichloromethane (LiChrosolv, MERCK), methanol (HPLC grade, POCh,) and acetonitrile (LiChrosolv, MERCK).

Photochemical reactions were carried out in quartz flasks using photoreactor prototype designed by Dariusz Wysiecki MSc., Eng. and constructed in cooperation with the Enviklim Company (Poland). The reactor is equipped with 3 UVA diode arrays (2×UV-D6565-4LED, 40 W and 1×UV-D6565-15LED, 150 W, λ = 365-370 nm).

^{1}H and ^{13}C NMR spectra were recorded on a Varian INOVA 500 spectrometer at 500 and at 125 MHz, respectively. Chemical shifts are reported in δ (ppm) units.

FTIR spectra (film and KBr pellet) were taken on Nicolet iS10 apparatus. High resolution mass spectra (HRMS) were taken on a SYNAPT G2-S HDMS (Waters) spectrometer with electrospray ionization source (ESI) and a TOF mass analyzer.

UV-Vis measurements were carried out with the use of an UNICAM UV 300 series spectrometer. Fluorescence spectra were recorded on a luminescence spectrometer (AMINCO Bowman Series 2 spectrofluorimeter) using the flash xenon lamp. The bandpass of excitation and emission monochromators was 16 nm. UV-Vis and fluorescence measurements were carried out in 1 cm quartz cuvettes. For measurements performed in mixed, water containing systems, deionized water (conductivity <1 $\mu S \cdot cm^{-1}$, Hydrolab, POLAND) was used.

Preparation. The reaction progress and purity of products were monitored by TLC using aluminum sheets covered with silica gel $60F_{254}$ (Merck). UV light (254 nm) was used as the detection method. Reaction mixtures were separated using a classical column (silica gel 60, 0.063-0.200 mm, Merck) or preparative thin layer (PLC plates, silica gel $60F_{254}$, 1mm, 20×20 cm size, Merck) chromatography. Reagent grade solvents were used.

Preparation of substrate for rearrangements - 19-azoxybenzocrown, 19-AZB-O

I. In a two-neck round-bottom flask acetone (110 mL), microgranules of NaOH (29.8 g, 0.745 mol) and 1,11-bis(2-nitrophenoxy)-3,6,9-trioxaundecane, podand **P-5O-NO_2**,[37] (11.53 g, 0.026 mol) are placed. To the vigorously stirred mixture a suspension of stannous chloride dihydrate (29.8 g, 0.157 mol) in water (90 mL) was added dropwise over 20 min. The reaction proceeded spontaneously in a turbulent manner. After the addition was complete,

the reaction mixture was refluxed for 30 minutes. Then toluene (ca. 200 mL) was added to the flask. The organic layer was separated and washed three times with water. The toluene extract was evaporated under reduced pressure. The mixture of macrocyclic compounds **19-AZB** (mainly) and **19-AZB-O** was isolated from the residue using classical column chromatography. At the beginning dichloromethane and next a mixture of dichloromethane with acetone (20:1 and 10:1, v/v) were used as eluents. Fractions with desired macrocyclic compounds were collected and the solvent was evaporated under reduced pressure. A mixture of crude macrocyclic compounds (5.9 g) was obtained with an estimated macrocyclization yield ~60%.

TLC: R_f (chloroform:methanol, 20:1): 0.51 (**19-AZB**); 0.58 (**19-AZB-O)**

II. A mixture of **19-AZB** and **19-AZB-O** obtained in the previous step (1.8 g, ~4.8 mmol calculated for the azocompound) dissolved in a mixture of acetic acid (16 mL) and 30% hydrogen peroxide (11 mL) was heated at 80 °C for 1.5 hour. After that time volataile components were evaporated under reduced pressure at a temperature up to 80°C. The residue was extracted with chloroform and the obtained extract was next washed with water several times. From the separated organic layer after solvent evaporation azoxycompound **19-AZB-O** was isolated by column chromatography using gradient separation: dichloromethane, its mixtures (v/v) with acetone: 50:1, 30:1 and 25:1. The pure product (1.3 g) crystallizes from 2-propanol; mp: 85-87 °C. ([37] - an oily product was obtained]).

^{1}H NMR (500 MHz, $CDCl_3$): δ= 3.59-3.61 (m, 4H), 3.65-3.68 (m, 4H), 3.91 (q, J = 5.2 Hz, 4H), 4.26-4.31 (m, 4H), 7.02-7.07 (m, 3H), 7.11 (d, J = 8.2 Hz, 1H), 7.3 (dt, J_1 = 8.5 Hz, J_2 = 1.5 Hz, 1H,), 7.42 (dt, J_1 = 8.2 Hz, J_2 = 1.5 Hz, 1H), 7.62 (dd, J_1 = 8.0 Hz, J_2 = 1.7 Hz, 1H), 8.07 (dd, J_1 = 8.3 Hz, J_2 = 1.5 Hz, 1H): FT-IR (KBr): ν=537, 547, 593, 738, 757, 842, 943, 998, 1043, 1069, 1087, 1127, 1170, 1227, 1251, 1288, 1333, 1349, 1440, 1453, 1474, 1492, 1602, 2873, 2903, 2952, 3079, 3097 cm^{-1}; FT-IR (film): ν=754, 844, 945, 1049, 1088, 1125, 1252, 1280, 1463, 1494, 1588, 1603, 2874, 2924, 3069 cm^{-1}; UV/Vis (acetonitrile): λ_{max} (ε) =236 (8700), 304 (5500), 336 nm (5800 $mol^{-1}dm^3cm^{-1}$).

Chemical rearrangement of 19-AZB-O – preparation of 19-*p*-OH

A two-neck round-bottom flask with **19-AZB-O** (1.0 g, 2.6 mmol), DMF (6 mL) was placed in a cooling (water/ice) bath. To the cooled mixture concentrated sulfuric acid (8 mL) was added slowly, dropwise with stirring (caution!). Then the mixture was heated in an oil bath at 90 °C for 30 min. When the reaction was completed, solid sodium carbonate was slowly (caution!) added in small portions to the cooled reaction mixture to partially neutralize the

acid. The rearrangement product was then extracted several times with dichloromethane. The combined organic layers were washed several times with water and the solvent was evaporated under reduced pressure. The residue was treated with 2-propanol and the precipitate was filtered off. A crude, yellow-brown product: **19-*p*-OH** (>90% purity) was obtained. The product of a higher purity was obtained by using classical column chromatography (eluent: mixture of dichloromethane:acetone, 3:1, v/v). Recrystallization from methanol gave the pure, orange compound (0.82 g, 82 %); mp: 104-105°C. TLC: R_f ($CHCl_3$:MeOH, 20:1): 0.38; (CH_2Cl_2:acetone, 10:1, v/v): 0.34.

Spectral properties (listed below) of the obtained product are in agreement with characteristics of **19-*p*-OH** obtained in a different way.[7]

^{1}H NMR (500 MHz, [D6]DMSO), azophenol tautomer: δ= 3.30-3.36 (m + water signals, 4H), 3.40-3.46 (m, 4H), 3.65-3.71 (m, 4H), 4.21-4.20 (m, 4H,), 6.41 (dd, J_1 = 8.3 Hz, J_2 = 2.0 Hz, 1H), 6.55 (d, J = 2.0 Hz, 1H), 6.93 (dd, J_1 = 7.8 Hz, J_2 = 2.0 Hz, 1H), 6.98 (t, J = 7.6 Hz, 1H), 7.09 (d, J = 8.8 Hz, 1H), 7.16 (d, J = 8.3 Hz, 1H), 7.35 (dt, J_1 = 7.6 Hz, J_2 = 2.0 Hz, 1H), 10.12 (s,1H); ^{1}H NMR (500 MHz, [D6]acetone), mixture of tautomers (QH 45%, AZ 55%), selected signals for the quinone-hydrazone form are given: δ= 5.93 (d, J = 1.5 Hz, 1H), 6.22 (dd, J_1 = 9.8 Hz, J_2 = 2 Hz, 1H), 11.8 (s, 1H); ^{13}C NMR (125 MHz, [D6]DMSO): δ= 68.6, 68.7, 68.7, 68.7, 70.3, 70.3, 70.5, 70.5, 101.4, 107.9, 114.4, 119.5, 120.3, 120.9, 130.4, 137.9, 145.5, 153.2, 156.6, 161.9; FT-IR (KBr): ν=1050, 1109, 1126, 1180, 1221, 1244, 1261, 1447, 1522, 1554, 1605, 1625, 3320, 3441 cm^{-1}; FT-IR (film): ν=754, 854, 950, 1046, 1107, 1239, 1263, 1447, 1448, 1519, 1602, 1622, 2921, 3071, 3301, 3417 cm^{-1}; UV/Vis (acetonitrile): λ_{max} (ε) =252 (11000), 340 (1000), 434 nm (16000 $mol^{-1}dm^3cm^{-1}$).

Photochemical rearrangement of 19-AZB-O

19-AZB-O in a quartz Erlenmeyer flask (typically 31-35 mg, input details in Table 2, Experimental) dissolved in the given solvent (65 mL per 35 mg of substrate) was subjected to UV irradiation for 75 min in the photoreactor. Within the timescale of the experiment the temperature of the solution was incresing up to ~70 °C. As a result of the reaction progress the color of the solution changed from light yellow to red-orange. After that time the mixture was quantitatively transferred to a round bottom flask to evaporate the solvent under reduced pressure. After dissolution in dichloromethane products of the photochemical rearrangement were isolated by preparative thin layer chromatography with a chloroform:methanol mixture (20:1 or 30:1, v/v) as the mobile phase. (Additional PLC

isolation of **19-al** from the mixture with **19-*o*-OH** in CH_2Cl_2:acetone (10:1) was conducted). The separated products were eluted from silica gel with a mixture of chloroform-methanol. After filtration and solvent evaporation the residue was dissolved in dichloromethane and filtrated one more time. Then the solvent was evaporated and the residue was weighed. Yields of photochemical rearrangement products: **21-*o′*-OH**, **19-*o*-OH**, **19-*p*-OH** and **19-al** are collected in Table 2.

Table 2. Inputs and yields of macrocyclic products obtained in photochemical rearrangements of **19-AZB-O**

Input	**19-AZB-O** [mg]	Solvent	Power [W]	Yield [mg] (yield) [%]				**19-AZBO** recovery [mg] (%)	Overall yield of isolated products of rearrangement [%]
				21-*o′*-OH	**19-*o*-OH**	**19-*p*-OH**	**19-al**		
A.	35.3	toluene	150	10.0 (28.3)	4.4 (12.2)	7.7 (21.8)	5.9 (16.7)	7.4 (21.0)	79.0
B.	32.7	DMF	148	2.0 (6.1)	14.0 (42.8)	3.0 (9.2)	6.7 (20.5)	7.0 (21.4)	78.6
C.	31.0	2-propanol	141	9.8 (32)	1.5 (5)	19.3 (62.0)	0.4 (1.0)	0 (0)	**100.0**
D.	34.2	n-butanol	141	7.0 (20.0)	7.0 (20.0)	4.3 (44.0)	4.2 (13.1)	0.9 (3.0)	**97.0**
E.	25.0	2-propanol/ acetic acid[a]	140	3.9 (16.0)	6.5 (26.0)	10.2 (41.0)	0	4.3 (17.0)	83.0
F.	32.4	xylene	144	12.0 (37.0)	5.2 (16.0)	10.0 (31.0)	3.2 (10.0)	2.0 (6.0)	**94.0**
G.	32.3	toluene/ acetic acid[a]	143	2 (6.0)	24.3 (75.0)	3.0 (9.0)	0	3.0 (9.0)	**90.0**
H.	32.4	toluene	95	7.8 (24.0)	2.9 (9.0)	3.6 (11.0)	4.5 (14.0)	13.6 (42.0)	58.0
I.	31.6	2-propanol	95	4.5 (14.0)	4.0 (13.0)	10.4 (33.0)	0	12.7 (40.0)	60.0
J.	125	toluene[b]	144	23.0 (24.9)	18.3 (19.8)	19.4 (21.0)	15.3 (16.6)	16.2 (17.5)	82.3

[a] 0.1 mL ; [b] 250 mL

Characterization of the products of photochemical rearrangement of 19-AZB-O

21-*o′*-OH

^{1}H NMR (500 MHz, [D6]DMSO), azophenol tautomer, δ= 3.34-3.36 (m + water signals, 4H), 3.41-3.43 (m, 2H), 3.60-3.62 (m, 2H), 3.66-3.68 (m, 2H), 3.74-3.76 (m, 2H), 4.19-4.22 (m, 2H), 4.40-4.42 (m, 2H), 6.61 (dd, J_1 = 9.0 Hz, J_2 = 2.7 Hz, 1H), 6.87 (d, J = 2.7 Hz, 1H), 7.10 (t, J = 8.1 Hz, 1H), 7.22 (d, J = 7.8 Hz, 1H), 7.45 (dt, J_1 = 8.7 Hz, J_2 = 1.5 Hz, 1H), 7.65-7.68 (m, 2H), 14.10 (s, 1H); ^{1}H NMR (500 MHz, [D6]acetone), azophenol tautomer, δ= 3.40-3.45 (m, 4H), 3.47-3.49 (m, 2H), 3.69-3.73 (m, 2H), 3.75-3.77 (m, 2H), 3.83-3.86 (m,

2H), 4.26-4.28 (m, 2H), 4.46 (t, *J*=3.8 Hz, 2H), 6.57 (dd, J_1 = 8.8 Hz, J_2 = 2.8 Hz, 1H), 7.00 (d, *J* = 2.7 Hz, 1H), 7.12 (dt, J_1 = 7.8 Hz, J_2 = 1.1 Hz, 1H), 7.23 (d, *J*=8.2, 1H), 7.46 (dt, J_1 = 8.0 Hz, J_2 = 1.7 Hz, 1H), 7.69 (d, *J* = 8.8 Hz, 1H), 7.75 (dd, J_1 = 7.7 Hz, J_2 = 1.1 Hz, 1H), 14.72 (s, 1H); ^{13}C NMR (125 MHz, [D6]DMSO): δ= 67.9, 69.8, 70.1, 70.2, 70.5, 70.7, 70.8, 71.6, 104.2, 110.5, 115.8, 116.0, 122.1, 131.4, 132.2, 134.3, 139.5, 154.7, 157.5, 163.5; FT-IR (KBr), ν=751, 862, 1044, 1108, 1128, 1185, 1252, 1282, 1324, 1457, 1485, 1497, 1615, 2915, 3441 cm^{-1}; FT-IR (film): ν= 753, 975, 1048, 1108, 1186, 1251, 1293, 1394, 1455, 1483, 1614, 2871, 2919, 3072, 3446 cm^{-1} (broad); HRMS (ESI): calcd for $C_{20}H_{24}N_2O_6$ $[M+Na]^+$: 411.1532, found 411.1523; mp: 137-138 °C (from hexane); TLC: R_f ($CHCl_3$:methanol, 20:1, v/v): 0.82. UV/Vis (acetonitrile): λ_{max} (ε) =395 nm (10000 mol^{-1}dm^{3}cm^{-1}).

19-*o*-OH

^{1}H NMR (500 MHz, [D6]DMSO) azophenol tautomer, δ= 3.15-3.18 (m, 4H), 3.30 (t, *J* = 5 Hz, 2H), 3.36 (t, *J* = ~4.5 Hz, 2H; partially overlapping with the water signal), 3.63-3.66 (m, 2H), 3.68-3.70 (m, 2H), 4.32-4.36 (m, 4H), 6.59 (d, *J*=8.3 Hz, 1H), 6.70 (d, *J* = 8.3 Hz, 1H), 7.12 (t, *J* = 7.3 Hz, 1H), 7.30 (d, *J* = 8.3 Hz, 1H), 7.31 (t, *J* = 8.3 Hz, 1H), 7.47 (dt, J_1 = 7.8 Hz, J_2 = 1.5 Hz, 1H); 7.51 (dd, J_1 =8.3 Hz, J_2 = 1.5 Hz, 1H), 13.33 (s, 1H); ^{1}H NMR (500 MHz, [D6]acetone) azophenol tautomer, δ= 3.18-3.20 (m, 4H), 3.33 (t, *J* = 5.5 Hz, 2H), 3.43 (t, *J* = 5 Hz, 2H), 3.71-3.73 (m, 2H), 3.78-3.80 (m, 2H), 4.41-4.44 (m, 4H), 6.60 (d, *J* = 8.5 Hz, 1H), 6.70 (d, *J*=8.2 Hz, 1H), 7.15 (t, *J* = 7.6 Hz, 1H), 7.30-7.34 (m, 2H), 7.48 (dt, J_1 = 7.8 Hz, J_2 = 1.6 Hz, 1H), 7.68 (dd, J_1 = 8 Hz, J_2 = 1.6 Hz, 1H), 14.05 (s, 1H); ^{13}C NMR (125 MHz, [D6]DMSO): δ= 69.7, 69.8, 69.9, 69.9, 70.2, 70.4, 70.8, 70.9, 107.0, 110.9, 117.6, 118.3, 122.2, 131.1, 132.3, 134.2, 142.3, 153.7, 155.3, 158.3; FT-IR (film), ν=757, 792, 947, 1109, 1247, 1288, 1454, 1480, 1593, 2869, 2925, 3065, 3485 cm^{-1} (broad); HRMS (ESI): calcd for $C_{20}H_{24}N_2O_6$ $[M+Na]^+$: 411.1532, found: 411.1526; mp: 79-80 °C (crystallizes in mass); TLC: R_f ($CHCl_3$:methanol, 20:1, v/v): 0.72. UV/Vis (acetonitrile): λ_{max} (ε) =363 nm (15000 mol^{-1}dm^{3}cm^{-1}).

19-al

^{1}H NMR (500 MHz, [D6]DMSO), two forms: δ= 3.11 (t, *J* = 5.2 Hz, 1.3H), 3.16 (t, *J* = 5.5 Hz, 1.3H), 3.25 (t, *J* = 5 Hz, 1.3H), 3.45 (t, *J* = 5 Hz, 1.3H), 3.57-3.66 (m, ~4.2H), 3.69-3.71 (m, 1.3H), 3.91 (t, *J*=5 Hz, 0.7H), 3.96 (t, *J*=5.2 Hz, 0.7H), 4.24-4.28 (m, ~2H), 4.35 (t, *J* = 5.2 Hz, 0.7H), 4.42-4.44 (m, 1.3H), 6.01-6.03 (m, 1H), 7.02-7.20 (m, 3H), 7.34 (d, *J* = 3.6 Hz, 0.35H), 7.48 (dd, J_1 = 7.7 Hz, J_2 = 1.5 Hz, 0.65H), 7.65 (dd, J_1 = 7.5 Hz, J_2 = 1.6 Hz, 0.35H), 7.81 (d, *J* = 4.1 Hz, 0.65H), 9.15 (s, 0.65H), 9.70 (s, 0.35H), 11.14

(s, 0.35H), 13.92 (s, 0.65H); ^{13}C NMR (125 MHz, [D6]DMSO): δ= 68.7, 69.0, 69.2, 69.8, 70.3, 70.5, 71.2, 71.4, 71.9, 72.8, 103.9, 113.0, 114.1, 118.0, 119.0, 122.0, 123.3, 124.7, 126.0, 141.2, 151.6, 182.6, 183.5; FT-IR (film), ν= 746, 938, 971, 983, 1055, 1148, 1207, 1257, 1403, 1457, 1484, 1517, 1551, 1577, 1654, 2882, 2942, 3020, 3080, 3104, 3311 (sharp) cm^{-1}; HRMS (ESI): calcd for $C_{20}H_{24}N_2O_6$ $[M+Na]^+$: 411.1532, found: 411.1528; mp: 144-145 °C TLC: R_f ($CHCl_3$:methanol, 20:1, v/v): 0.68; (CH_2Cl_2:acetone, 10:1, v/v): 0.34; UV/Vis (acetonitrile): λ_{max} (ε) =425 nm (25000 $mol^{-1}dm^3cm^{-1}$).

19-*p*-OH

The properties of the compound obtained in photochemical rearrangement were identical with the properties of the product obtained in a reaction analogous to the Wallach rearrangement.

X-ray crystal structure determination

Diffraction data were collected on an IPDS 2T dual-beam diffractometer (STOE & Cie GmbH) at 120.0(2) K with Mo K_α radiation of the microfocus X-ray source (GeniX 3D Mo High Flux, Xenocs, 50 kV, 1.0 mA, λ = 0.71069 Å). The crystal was thermostated in a nitrogen stream at 120 K using the CryoStream-800 device (Oxford CryoSystem) during the entire experiment. Data collection and data reduction were controlled by the X-Area 1.75 program (STOE).

Deposition Numbers 1940852 (for 2**1-*o′*-OH**), 1973355 (for **19-al**) contain the supplementary crystallographic data for this paper. These data are provided free of charge by the joint Cambridge Crystallographic Data Centre and Fachinformationszentrum Karlsruhe Access Structures service www.ccdc.cam.ac.uk/structures.

21-*o′*-OH

Single crystals of **21-*o′*-OH** suitable for X-ray analysis were obtained by slow evaporation of methanol from solution.

An absorption correction was performed on the integrated reflections by a combination of frame scaling, reflection scaling and spherical absorption correction. Outliers have been rejected according to Blessing's method. The structures were solved by direct methods and refined anisotropically using program packages OLEX 2[47] and SHELX-2015[48]. Positions of hydrogen atoms were calculated geometrically and taken into account with isotropic temperature factors. Computer programs: *X-AREA* WinXpose 2.0.22.0 (STOE, 2016), *X-AREA* Recipe 1.33.0.0 (STOE, 2015), *X-AREA* Integrate 1.72.0.0 (STOE, 2018) *X-AREA X-*

RED32 1.63.4.0 (STOE, 2017), *SHELXS*,[49] *SHELXL*, [48] Olex2.[47]

Crystallographic details are collected in Supporting Information.

19-al

Single crystals of **19-al** suitable for X-ray analysis were obtained by slow evaporation of acetone from solution.

Due to a low absorption coefficient no absorption correction was performed. The structure was solved using intrinsic phasing implemented in SHELXT and refined anisotropically using program packages OLEX2 [47] and SHELX-2015.[48] Positions of the C–H hydrogen atoms were calculated geometrically taking into account isotropic temperature factors. All H-atoms were refined as riding on their parent atoms with the usual restraints.

Special treatment. Structure **19-al** was refined with disorder of the whole molecule (Figure S10). Only etheric parts are common for the two orientations of molecules. The 5-membered and 6-membered aromatic rings exchange their positions, together with the -NHN- group, with site occupation factors of 0.569(7)/0.431(7) for different orientations forming O1-C6 and O5-C15 or otherwise O1-C15A and O5 C6a, compare the scheme below.

Structure determination of 21-*o'*-OH and 19-al in solution

1D ^{1}H NMR spectra were collected with standard parameters (45° pulse length 3.9 μs and the delay time 1 s).

The 2D NMR spectra of **21-*o'*-OH** were recorded at 32 °C and a sample concentration of 10 mg/ml. The measurement temperature was higher to shift the water signal overlapping with the compound signals. The ROESY spectrum was collected in the phase-sensitive mode with a spectral width of 6546 Hz and a mix time of 80 ms in a 4320×330 matrix with 8 accumulations per increment in a 4K×1K matrix. The spectral windows of the **21-*o'*-OH** HSQC spectrum for ^{1}H and ^{13}C of axes were 7207 Hz and 21362 Hz, respectively. The data were collected in a 2882×200 matrix and processed in a 4K×1K matrix. The spectral windows of **21-*o'*-OH** HMBC spectrum for ^{1}H and ^{13}C axes were 7207 Hz and 251341 Hz, respectively. The data were collected in a 2162 × 240 matrix and processed in a 4K × 1K matrix.

The 2D NMR spectra of **19-al** were recorded at ambient temperature and a sample concentration of 10 mg/ml. The ROESY spectrum was collected in the phase-sensitive mode with a spectral width of 7997 Hz and a mix time of 80 ms in a 5278×330 matrix with 8

accumulations per increment in a 4K×1K matrix. The HSQC and HMBC experiments of all samples were performed with pulse field gradients. The HSQC spectra were acquired in the phase-sensitive mode with 1J(CH) set to 146 Hz. The HMBC spectra were acquired in the absolute value mode with nJ(CH) set to 8 Hz. The spectral windows of **19-al** HSQC spectrum for ^{1}H and ^{13}C of axes were 7323 Hz and 23873 Hz, respectively. The data were collected in a 2930 × 210 matrix and processed in a 4K×1K matrix. The spectral windows of **19-al** HMBC spectrum for ^{1}H and ^{13}C axes were 7997 Hz and 23881 Hz, respectively. The data were collected in a 3998×220 matrix and processed in a 4K×1K matrix.

Metal cation interaction studies

Complexation studies were performed by spectrophotometric titration of the crown solution in acetonitrile with the respective metal perchlorate (for metal cations). *Caution! Perchlorate salts should be regarded as potentially explosive and handled with care.* The stock solutions of azobenzocrowns (~10^{-4} M) and metal perchlorates, TBAOH, *p*-toluenesulfonic acid (~10^{-2} M) were prepared by weighing their respective quantities and dissolving in acetonitrile in volumetric flasks. For titrations, azobenzocrown solutions of 2.3 mL starting volume in the cuvette were used. The stability constant values from UV-Vis experiments were calculated with the use of the OPIUM[50] program.

For evaluation of binding constant K from fluorescence measurements, where quenching of fluorescence was observed the following equation was applied:

$$F_0/(F-F_0)= [a/(b-a)][1/K[M] +1]$$

The stability constant was determined as the intercept (b)/slope (a) ratio from the plot $F_0/(F-F_0)$ versus $[M]^{-1}$. F_0 is the fluorescence intensity of hydroxyazobenzocrown, F - the fluorescence intensity in the presence of metal perchlorate or TBAOH, [M] - salt concentration.

Binding constants for cases where fluorescence increase was observed were obtained by using the original Benesi-Hildebrand method[51] adapted for fluorescence measurements. The binding constant was obtained by the graphical method as the intercept/slope ratio of linear relationship $c_{crown}/F = f(1/c_{salt})$, where c_{crown} and c_{salt} are crown ether and metal perchlorate concentration [M], respectively F is the fluorescence intensity value.

Stern-Volmer constants K_{sv}[43] were determined graphically according to equation:

$$F_0/F=1+K_{SV}[Q]$$

where F_0 is the fluorescence intensity in the absence of quencher, F – fluorescence intensity in the presence of quencher, [Q] - quencher (metal perchlorate, triethylamine, TBAOH] concentration [M].

Protonation constants determination

The stock solutions, for working solutions preparation, of the crowns (~10^{-4} M) and *p*-toluenesulfonic acid (~10^{-2} M) were prepared by weighing the respective quantities of substances and dissolving them in volumetric flasks in acetonitrile. Azobenzocrowns working solutions (2.3 mL) were titrated with a solution of *p*-toluenesulfonic acid. The protonation constant values from UV-Vis titrations were estimated from titration data, analogously to stability constants of complexes, with the use of the OPIUM[50] program. Binding constants from fluorescence experiments were obtained by using the original Benesi-Hildebrand method[51] adapted to fluorescence measurements. The proton binding constant was obtained by the graphical method as the intercept/slope ratio of linear relationship $c_{crown}/F = f(1/c_{TosOH})$, where c_{crown} and c_{TosOH} are crown ether and *p*-toluenesulfonic acid concentration [M], respectively, F is the fluorescence intensity value. Given average values were obtained from two independent measurements.

Acknowledgments

This work was supported by an internal grant from statutory funds of the Faculty of Chemistry, Gdańsk University of Technology No. 033150.

Conflict of Interest

The authors declare no conflict of interest.

Keywords: macrocycles • photochemistry • rearrangement • supramolecular chemistry • tautomerism

[1] G.S. Kumar, *Azo Functional Polymers: Functional Group Approach in Macromolecular Design*, CRC Press, Lancaster, **1992**.

[2] R.W. Sabnis, *Handbook of Acid-Base Indicators*, CRC Press, London, **2008**.

[3] E. Luboch, R. Bilewicz, M. Kowalczyk, E. Wagner-Wysiecka, J.F. Biernat, in *Advances in Supramolecular Chemistry*: *Azo Macrocyclic Compounds*, Vol. 9 (Ed. G.W. Gokel) Cerberus Press, South Miami, **2003**, pp. 71–162.

[4] E. Wagner -Wysiecka, N. Łukasik, J.F. Biernat, E. Luboch, *J. Incl. Phenom. Macrocycl. Chem.* **2018**, *90*, 189–257.

[5] M. Shiga, H. Nakamura, M. Takagi, K. Ueno, *Bull. Chem. Soc. Jpn*. **1984**, *57*, 412–415.

[6] R. Tahara, T. Morozumi, H. Nakamura, M. Shimomura, *J. Phys. Chem. B.* **1997**, *101*, 7736–7743.

[7] E. Luboch, E. Wagner-Wysiecka, Z. Poleska-Muchlado, V.Ch. Kravtsov, *Tetrahedron* **2005**, *61*, 10738–10747.

[8] E. Luboch, *Pol. J. Chem*. **2008**, *82*, 1315–1318.

[9] E. Luboch, E. Wagner-Wysiecka, T. Rzymowski, *Tetrahedron* **2009**, *65*, 10671–10678.

[10] M. Szarmach, E. Wagner-Wysiecka, M.S. Fonari, E. Luboch, *Tetrahedron* **2012**, *68*, 507–515.

[11] M. Szarmach, E. Wagner-Wysiecka, E. Luboch, *Tetrahedron* **2013**, *69*, 10893–10905.

[12] E. Wagner-Wysiecka, M. Szarmach, J. Chojnacki, N. Łukasik, E. Luboch *J. Photochem. Photobiol. A- Chem.* **2017**, *333*, 220–232.

[13] L. Antonov (Ed.), *Tautomerism: Methods and Theories*, Wiley-VCH Verlag GmbH & Co. KGaA, **2013**.

[14] O. Wallach, L. Belli, *Ber. Dtsch. Chem. Ges*. **1880**, *13*, 525–527.

[15] I. Shimao, *Nippon Kagaku Kaishi* **1985**, *8*, 1556-1559 (in Japan).

[16] A. Lalitha, K. Pitchumani, C.J. Srinivasan, *J. Mol. Catal. A: Chem.* **2000**, *160*, 429–435.

[17] M.M. Shemyakin, V.I. Maimind, B.K. Vaichunaite, *Russ. Chem. Bull.* **1963**, *12*, 808–812.

[18] M.M. Shemyakin, Ts.E.Agadzhanyan, V.I. Maimind, R.V. Kudryavtsev, *Russ. Chem. Bull*. **1963**, *12*, 1216–1219.

[19] G.A. Olah, K. Dunne, D.P. Kelly, Y.K. Mo, *J. Am. Chem. Soc.* **1972**, *94*, 7438–7447.

[20] R.A. Cox, E. Buncel, *J. Am. Chem. Soc*. **1975**, *97*, 1871–1875.

[21] R.A. Cox, E. Buncel, The Chemistry of the Hydrazo, Azo and Azoxy Groups Vol. 1 (Ed. S. Patai), John Wiley & Sons, Ltd., **1975**, pp. 775–859.

[22] J. Yamamoto, T. Sakamoto, K. Kusunoki, M. Umezu, T. Matsuura, *Nippon Kagaku Kaishi* **1977**, *1*, 66–71 (in Japan).

[23] J. Yamamoto, N. Tanaka, M. Yamamoto, T. Nakagawa, H. Aim, *Nippon Kagaku Kaishi* **1987**, *5*, 851–857 (in Japan).

[24] S. Oae, T. Fukumoto, M. Yamagami, *Bull. Chem. Soc. Jpn.* **1963**, *36*, 601–605.

[25] C.S. Hahn, H.H. Jaffe, *J. Am. Chem. Soc*. **1962**, *8*, 946–949.

[26] E. Buncel, *Acc. Chem. Res.* **1975**, *8*, 132–139.

[27] G.M. Badger, R.G. Buttery, *J. Chem. Soc*. **1954**, 2243–2245.

[28] G.E. Lewis, J.A. Reiss, *Aust. J. Chem.* **1966**, *19*, 1887–95.

[29] G.G. Spence, E.C. Taylor, O. Buchardt, *Chem. Rev*. **1970**, *70*, 231–265.

[30] N.J. Bunce, Can. J. Chem. **1977**, *55*, 383–392.

[31] A. Albini, E. Fasani, M. Moroni, S. Pietra, *J. Org. Chem*. **1986**, *51*, 88–92.

[32] H. Shine, W. Subotkowski, E. Gruszecka, *Can. J. Chem*. **1986**, *64*, 1108–1115.

[33] M. Okubo, H. Hyakutake, N. Taniguchi, *Bull. Chem. Soc. Jpn.* **1988**, *61*, 3005–3007.

[34] A. Bhatnagar, A. Schroder, D.K. Mohanty, *Polymer* **1997**, *38*, 239–243.

[35] T. Issiki, H. Miyagawa, H. Sasaiu, J. Yamamoto, *Nippon Kagaku Kaishi* **1997**, *3*, 207–212 (in Japan).

[36] J. Yamamoto, R. Hamada, T. Tsuboi, *Nippon Kagaku Kaishi* **2002**, *3*, 339–343 (in Japan).

[37] A.M. Skwierawska, J.F. Biernat, V.Ch. Kravtsov, *Tetrahedron* **2006**, *62*, 149–154.

[38] P.P. Boule, C. Guyon, J. Lemaireboule, *Chemosphere* **1982**, *11*, 1179–1188.

[39] Ch. Reichardt, *Solvents and Solvent Effects in Organic Chemistry*, Third Edition, Verlag GmbH & Co. KGaA, Weinheim, p. 118.

[40] E. Luboch, E. Wagner-Wysiecka, J.F. Biernat, *J. Supramol. Chem*. **2002**, *2*, 279–291.

[41] E. Luboch, V.Ch. Kravtsov, *J. Mol. Struct.* **2004**, *669*, 9–15.

[42] M. Muroi, A. Hamaguchi, E. Sekido, *Anal. Sci.* **1986**, *2*, 351–356.

[43] J.R. Lakowicz, *Principles of Fluorescence Spectroscopy*, New York: Kluwer Academic/Plenum, 3rd Ed. **2006**.

[44] J. Do Choi, R. D. Fugate, P.S. Song, *J. Am. Chem. Soc.* **1980**, *102*, 5293–5297.

[45] R.B. Orfão Jr., F. de Carvalho, P. Homem-de-Mello, F.H. Bartoloni, *J. Braz. Chem. Soc.* **2017**, *28*, 1896–1904.

[46] E. Luboch, J.F. Biernat, Yu.A. Simonow, V.Ch. Kravtsov, V.K. Bel'skii, *Supramol. Chem.* **1999**, *11*, 109–118.

[47] O.V. Dolomanov, L.J. Bourhis, R.J. Gildea, J.A.K. Howard, H. Puschmann, *J. Appl. Cryst.* **2009**, *42*, 339–341.

[48] G.M. Sheldrick, *Acta Crystallogr*. **2015**, *C 71*, 3–8.

[49] G.M. Sheldrick, *Acta Crystallogr*. **2008**, *A64*, 112–122.

[50] M. Kyvala and I. Lukeš, program package ”OPIUM” available (free of charge) at http://www.natur.cuni.cz/~kyvala/opium.html.

[51] H.A. Benesi, J.H. Hildebrand, *J. Am. Chem. Soc.* **1949**, *71*, 2703–2707.

Table of Contents entry

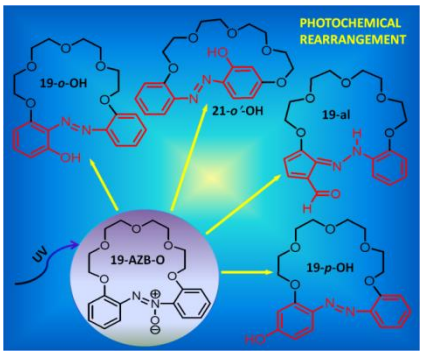

"Smart UV" - interesting macrocyclic products in one-pot process. Photochemical rearrangement of 19-membered azoxybenzocrown (**19-AZB-O**) results in formation of macrocyclic compounds, including three hydroxyazobenzocrowns. Macrocycles can be obtained, depending on conditions, with high, even over 70%, yield. The structures of two atypical products **21-*o*′-OH** and **19-al** were determined in the solid state (X-ray) and in solution (NMR). Tautomeric equilibrium of hydroxyazobenzocrowns and its change depending on acidity/basicity of the environment and metal cation complexation were studied using spectroscopic methods.